



ANALYSIS OF POSSIBLE MAGNET RELATED CAUSES OF THE TEVATRON TUNE AND COUPLING DRIFT AND SNAPBACK DURING INJECTION

G. Annala, P. Bauer¹, R. Berggreen, J. DiMarco, H. Glass, R. Hanft,
D. Harding, M. Lamm, M. Martens, T. Sager, P. Schlabach,
M. Tartaglia, J.C. Tompkins, G. Velez

Fermilab

Tune and coupling drift were observed by Annala and Martens in the Tevatron during the initial stages of run II. Using standard formulae the observed tune drift over two hours on the injection porch can be correlated with a total of ~ 100 units (of 10^{-4} times the dipole field at injection) of quadrupolar field over the entire ring. This indicates a small effect, which can be produced by one (normal $-b_1$ - or skew $-a_1$ -) corrector quad running at ~ 7 A. The time-dependence of the tune and coupling drift is logarithmic, similar to that of the sextupole (b_2) drift in the main dipoles. It is therefore suspected that the cause of the problem lies within the main superconducting magnets of the Tevatron. The following note discusses the tune drift issue in the Tevatron, and explores possible avenues of explanation. These are a) feed-down effects from the sextupole fields in the main dipoles and sextupole correctors due to beam-offset and/or systematic magnet misalignment and geometric errors; b) possible wiring errors in the corrector circuits, c) possible decaying main fields in quadrupoles and d) decaying skew and normal quadrupole components in the main dipoles.

Table of Content

- 1) Introduction
- 2) Tune & Coupling (static & drift) Issues in the Tevatron
 - 2.1) Summary of a_1/b_1 beam studies
 - 2.2) Calculation of the a_1/b_1 strength causing the drift effects
- 3) Summary a_1 - b_1 measurements in MTF
 - 3.1) Geometric a_1/b_1
 - 3.2) Hysteretic a_1/b_1
 - 3.3) Geometric a_1/b_1 on the ramp
 - 3.4) Dynamic a_1/b_1
- 4) Magnet-based models for tune & coupling in Tevatron, incl. drift
 - 4.1) Non feed-down scenarios
 - 4.2) Basics on b_2 in Tevatron dipoles to understand feed-down
 - 4.3) Feed-down scenarios
- 5) Summary

¹ e-mail: pbauer@fnal.gov

1) Introduction

Tune (and coupling) drift were first observed in the spring and summer of 2002 by Annala and Martens in the Tevatron during the injection porch². The tune drift is followed by a fast tune perturbation at the start of the ramp, possibly a result of the tune snapback. The tune perturbations at the start of the ramp are believed to exacerbate emittance growth and beam loss. Tune and coupling in circular accelerators are the result of normal (b_1) and skew (a_1) quadrupole fields in its lattice. The following explores possible sources of drifting quadrupolar fields in the Tevatron, with particular emphasis on the superconducting main dipoles.

Chapter 2 summarizes recent tune and coupling drift measurements in the Tevatron. As will be shown in this chapter the observed tune drift is explained with a very weak quadrupole field component, if evenly distributed over the ring. The change of tune following a 1-2 hr drift, for instance, can be produced by only one Tevatron corrector quadrupole.

Chapter 3 summarizes our current knowledge of the normal and skew quadrupole (and drift) in the superconducting magnets of the Tevatron derived from results of former and recent magnetic measurement campaigns. The discussion encompasses not only dynamic, but also geometric and hysteretic a_1/b_1 components. The most important part of this chapter is the discussion of intrinsic dynamic a_1/b_1 components in Tevatron dipoles.

Chapter 4 finally explores possible avenues of explanation for the tune and coupling drift. These avenues are a) feed-down effects from the sextupole fields in the main dipoles and sextupole correctors due to beam-offset and/or systematic magnet misalignment; b) possible wiring errors in the corrector circuits, c) possible decaying main fields in quadrupoles and d) decaying skew and normal quadrupole components in the main dipoles. Since feed-down effects are those most discussed, this chapter first introduces the static and dynamic properties of the sextupole component in the superconducting dipole magnets in the Tevatron. More on the sextupole drift can be found in a recently published note (TD-04-043 or reference [10]).

² It appears that tune perturbations were also observed during run-I, although the consequences were apparently less dramatic and the issue was never pursued further (and no explicit measurement of the tune drift from that time exists). In the current run-II, the beam intensity is significantly increased and with it the tune spread. There appears to be no indication, however, that the tune drift and tune snap-back are by any means more pronounced in run-II than in run-I.

2) Tune and Coupling Drift in the Tevatron

The following summarizes a set of beam-based measurements that were performed in the Tevatron to understand the tune perturbations observed during ramping from injection. These beam studies are described in further detail in various internal notes. Both [1] and [2] describe the initial measurements, which established the tune drift effect for the first time during the summer of 2002. Both also give a description of RF frequency vs tune measurements, which allow determination of the average beam orbit in the sextupole correctors. The results of these measurements play a crucial role in our understanding of tune drift today. Reference [3] contains a detailed description of the sextupole and quadrupole correction algorithms derived from the 2002-2004 tune drift and magnet sextupole decay measurements. In 2002 a dedicated tune and coupling drift compensation feed-forward system was first implemented into the Tevatron normal and skew quadrupole corrector protocol. These initial feed-forward algorithms are described in [4] and [5]. Reference [6] documents the latest series of tune and coupling drift measurements, conducted during the summer of 2004. Note that at that time the tune and coupling drift changed with respect to 2002 and a new feed-forward algorithm needed to be implemented. The cause(s) of tune and coupling drift in the Tevatron, however, remain(s) to be understood and it is the purpose of this document to discuss the most plausible explanations.

2.1) Tune and Coupling Drift Measurements in the Tevatron

The plot in Figure 1 shows the non-integer part of the horizontal and vertical tunes during the injection porch, as measured with the Schottky monitors on 05/15/2002 [1]. The horizontal tune drifts from 20.595 to ~20.585. This is significant, corresponding to 2.5 % of the fractional tune ($0.015/0.595=0.025$). Prior to each of the tune measurements shown in Figure 1, the tunes were decoupled using the skew trim quads. After decoupling, the tunes were split as far as necessary using the trim quad circuits ($q_v=0.56$ and $q_h=0.59$) to prevent interference of coupling effects (occurring when the tunes have drifted toward the minimum tune split). The standard fractional operating tunes in the Tevatron are $q_v=0.575$ and $q_h=0.583$. The closest resonances lie at 0.6 and 0.571. Interestingly the vertical tune in Figure 1 drifts by 60% more than the horizontal tune. A possible explanation is that it is the result of precision of the measurements. It is possible that the coupling-drift caused coupling of the tunes to be re-introduced despite the measures taken to prevent the effect. Similar measurements conducted in 2004 (Figure 5) do not have this feature. The tune drift measurement, however, was found to be reproducible (3 different sets of measurements performed on three different days).

The observed tune drift is believed to be related to the subsequent tune snap-back. The tune “water-fall” plot of the start of the ramp shown in Figure 2 reveals that the sign and magnitude of the “outward” tune snap-back is consistent with a reversal of the effects of

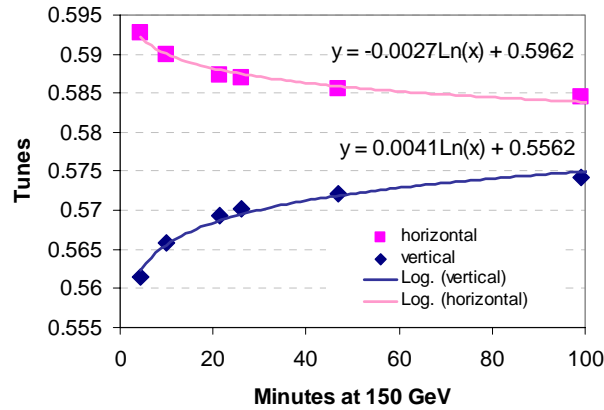


Figure 1: Tevatron tune drift during the injection plateau, measured on 05/15/2002.

the tune drift. The measurements shown in Figure 1 were performed with 30-bunch, un-coalesced (low intensity) proton beams on the “center-orbit” (with the helix switched off). As in standard operation, the sextupole decay in the dipoles during the injection porch was compensated by the sextupole corrector circuits. The chromaticity was indeed flat during the injection porch as shown by dedicated measurement.

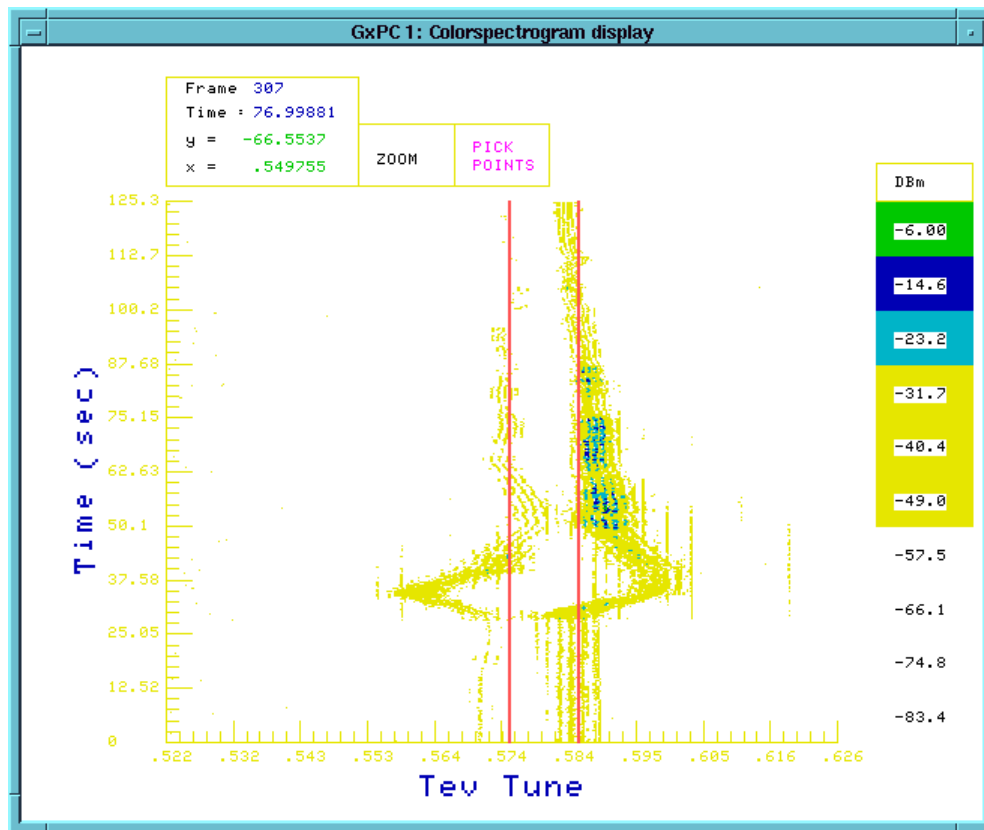


Figure 2: Recorded Tevatron tunes during the start of the ramp after injection. The particular parameter sets during the ramp shown here is unknown. The sudden changes in the horizontal and vertical tunes at the start of the ramp are probably a snapback.

Figure 3 is a plot of the change in the skew quad circuits T:SQ (42 quads) and T:SQA0 (2 quads) needed to decouple the Tevatron as a function of time at 150 GeV, also taken from a measurement performed on 07/10/2002 [2]. As before with the tune drift experiments the measurements were performed with protons only, with the helix switched off. The measured data points are shown together with a logarithmic fit. Note that the T:SQ circuit provides 13 times as much coupling per amp than the T:SQA0 circuit. In these measurements the tunes were decoupled to the level of minimum tune split of about 0.002 units at the beginning of the injection porch. A MAD calculation on the basis of the Tevatron design lattice and the known strength of the magnets in the T:SQ circuit gives a coupling of 0.106 units of minimum tune split per amp in T:SQ. Thus the measured change of about 0.2 amps in T:SQ needed to decouple the Tevatron is consistent with a minimum tune split of about 0.02 units.

Figure 4 shows the measured minimum tune split as a function of time at 150 GeV. The measured data points are shown and the line is a logarithmic fit function. The skew trim quads were set such as to decouple the machine at the beginning of the measurement. Then, these settings were left unchanged during the measurements. The tune trim quads were used to shift the tunes toward each other until the minimum tune split condition was found. The tune quads were reset to their initial state after each measurement. Similarly to Figure 3 the result of the measurement shown in Figure 4 reveals a logarithmic coupling drift during the injection porch. The time dependent coupling is an indication of a time dependent skew quadrupole in the ring. An order of magnitude estimate of the coupling drift is given in 2.2.

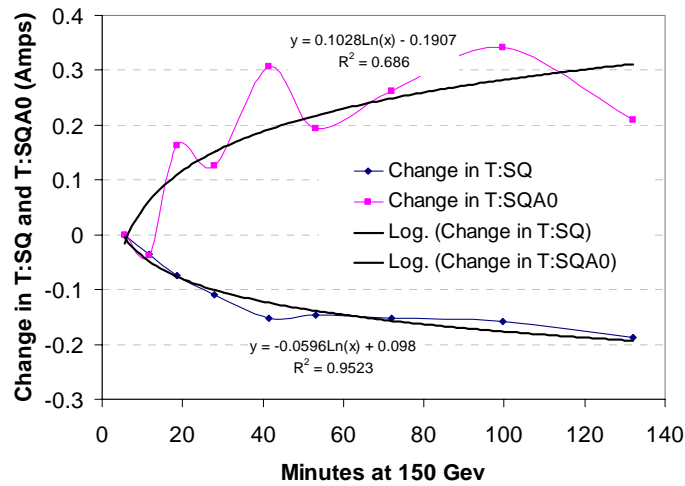


Figure 3: Current in skew quadrupole circuits to keep machine de-coupled. Note that the T:SQ circuit comprises 42 magnets, whereas the T:SQA0 circuit consists of only two correctors. Measurement 07/10/02 [1].

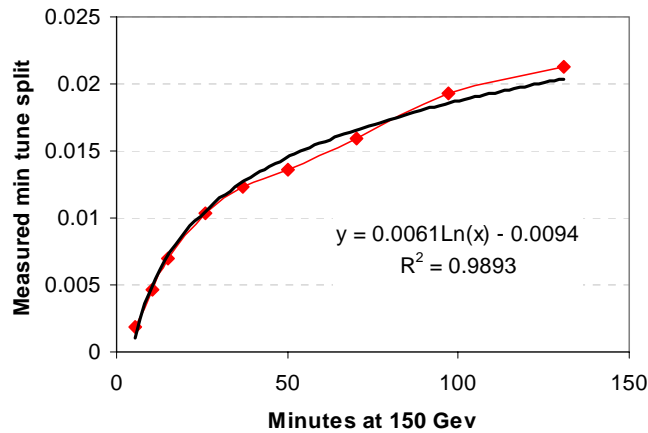


Figure 4: Minimum tune split in Tevatron during injection plateau. Measurement 07/10/02 [1].

Several re-shimming campaigns conducted during January and October 2004 were intended to reduce the (static) coupling in the Tevatron, which had appeared over the years as a result of suspension creep in the main dipoles [18]. This creep caused a drop of the coils within the warm iron yoke, inducing an up-down imbalance (or skew quadrupole moment) in the contribution of the iron yoke to the dipole field in the bore of the magnet. The re-shimming campaigns reduced coupling in the machine. Note that during 2004 the beam-less pre-cycle was modified in the context of improvements of the sextupole drift and snapback compensation [19]. This change consisted in an increase of the pre-cycle flat-top from ~30 mins to 1hr or more and an increase of the back-porch from 1 min to 5 mins. Either as a result of reduced coupling or the changes in the pre-cycle the drift behavior was also affected by the shut-downs and new feed-forward algorithms needed to be devised during start up of Tevatron after each of the re-shimming campaigns. The latest tune and coupling drift studies were conducted in the Tevatron in Aug. 2004.

Figure 5 presents the results of these recent tune drift measurements. Since the tune drift was already corrected with the feed-forward tune-drift algorithm implemented in 2002 the corrected tune drift was added to the measured tune drift to obtain the results shown in the figure. Figure 6 shows the coupling drift measured. The plot also contains the skew quad corrector supplied coupling.

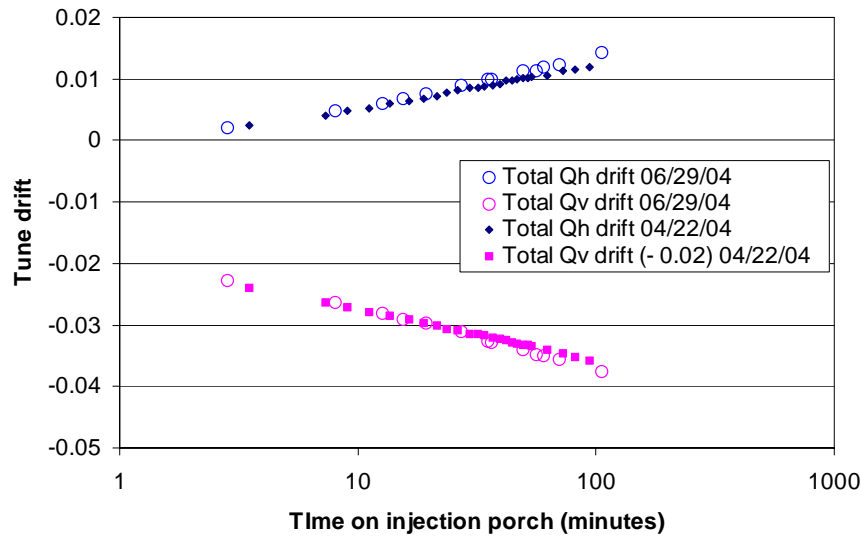


Figure 5: Total horizontal and vertical tune drift derived from the tune drift measured on 06/29/2004 with un-coalesced protons-only beam on center orbit following a 25.6 hrs flat-top and 5 min back-porch. Also shown are the data from 04/22/04 (with the vertical drift data were shifted by -0.02 units).

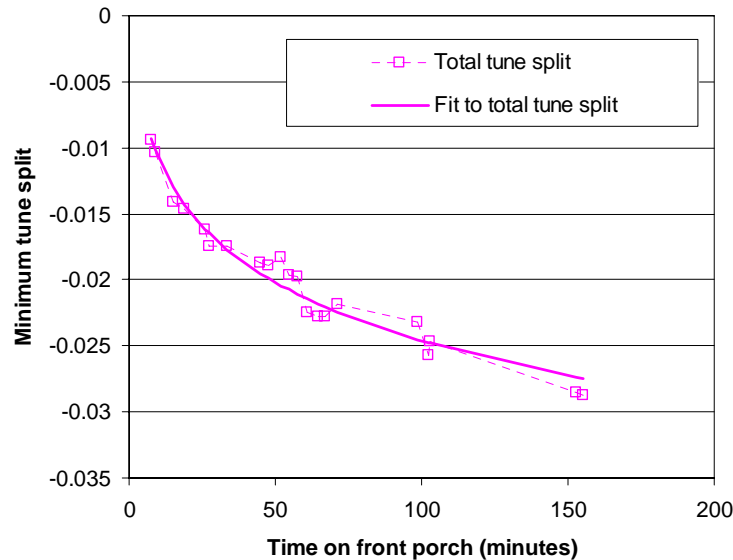


Figure 6: Amount of coupling drift on the front porch during the 7/23/04 studies. The open squares are the estimated total amount of coupling drift based on the measured tune split and the solid line is a fit to the coupling drift.

The following aspects of the Tevatron tune and coupling drift are noteworthy:

- a) The tune, coupling and sextupole drifts in the superconducting Tevatron dipoles during the injection porch are all characterized by a logarithmic dependence on time

passed on the injection porch. Figure 7 shows that the sextupole corrector currents can, by proper transformation, easily be superimposed on the tune drift data. Unfortunately that does not necessarily mean that the tune drift has exactly the same time constant as the chromaticity drift. When converting the logarithmic (fractional) tune function to the current a conversion coefficient is used. This coefficient has no physical meaning and cannot be calculated from first principles. Unfortunately there is always the possibility to move part of the coefficient into the argument of the log function where it could affect the time constant.

- b) The horizontal and vertical drift (see Figure 1) are approximately of the same magnitude but of opposite sign. This could be an indication that the cause of the problem resides within one “type” of magnet. If the cause of the phenomenon resides in the main dipoles (as a result of feed-down from their decaying sextupole fields, for instance), one would expect the time changing quadrupole fields seen by horizontally off-set beams to be of the focusing kind horizontally and defocusing vertically, which corresponds to what is observed.

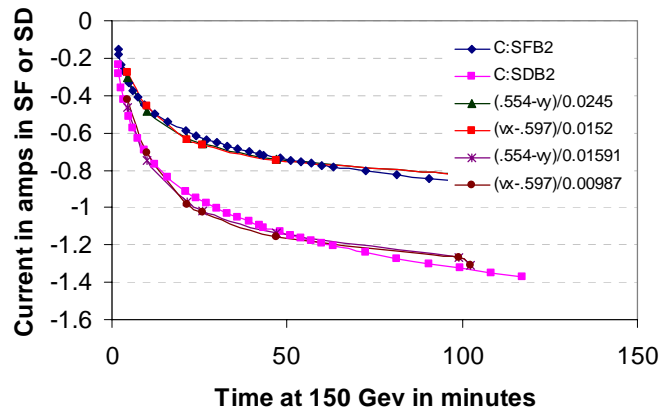


Figure 7: Sextupole correction currents and fit of tune drift data (August 2002 beam study).

2.2) Order of Magnitude Estimate

The following is an attempt to compute the normal and skew quadrupole strengths required to generate the experimentally observed tune and coupling drifts during injection. Note that the quadrupoles are calculated in units of dipole field and are therefore the total units that have to be put into one dipole to generate the effects discussed. Obviously this number of units can also be divided by the total number of 773 dipoles in the Tevatron to estimate the number of units per magnet in a distributed scheme.

The horizontal tune change, Δq_x , from a changing quadrupole magnetic field with length integrated strength $\Delta K_l L$ is given by:

$$\Delta q_x = \frac{1}{4\pi} \beta_x \Delta K_1 L, \quad (2)$$

where ΔK_1 is the change in transverse kick factor, which is the gradient normalized to the dipole bending strength, $B\rho$. For a known tune shift (between start and end of the drift at the injection porch) of 0.015 the (length integrated) kick factor $\Delta K_1 L$ needed, is (the horizontal β -function in the Tevatron dipoles is 57.4 m):

$$\Delta K_1 L = \frac{4\pi \Delta q_x}{\beta_x} = 3.3 \cdot 10^{-3} \frac{1}{m} \quad (3)$$

The kick strength K_1 can be related to a quadrupole field B_1 , or more specifically, a gradient G , with $B\rho$ ($\sim 500 \text{ Tm}$), the dipole bending strength at injection:

$$\Delta G \cdot L = B\rho \cdot \Delta K_1 L = 1.65 \left(\frac{T}{m} m \right) \quad (4)$$

This length integrated gradient divided by the dipole magnetic length of 6.12 m gives a total gradient of $G=0.266 \text{ T/m}$. This gradient can be converted into a quadrupole coefficient, b_1 , in “units” of dipole field B_0 (0.66 T at injection!) with (the reference radius $r_0=1 \text{ inch}$):

$$b_1 = \frac{Gr_0}{B_0} 10^4 = 102 \text{ units} \quad (5)$$

This can be compared to the measurement of the change in (corrector-) quadrupole required to compensate for the total tune drift. The tune change generated by one corrector quadrupole (75 kG-in @ 1”, 50 A), as calculated by M. Martens, is 0.0022/A [1]. Therefore 6.82 A are required in one quadrupole corrector to produce the observed 0.015 tune shift.

An order of magnitude estimate of the skew quadrupole can also be derived from the tune-split measurement shown in Figure 4. A change in minimum tune split, $\Delta \nu_{min}$, is defined by:

$$\Delta C_{sq} = \frac{1}{2\pi} \sum (K_1 L)_{sq,i} \sqrt{\beta_{x,i} \beta_{y,i}} \cos(\phi_y - \phi_x) \quad (6)$$

$$\Delta S_{sq} = \frac{1}{2\pi} \sum (K_1 L)_{sq,i} \sqrt{\beta_{x,i} \beta_{y,i}} \sin(\phi_y - \phi_x) \quad (7)$$

$$\Delta \nu_{min} = \sqrt{\Delta C_{sq}^2 + \Delta S_{sq}^2} \quad (8)$$

A change in tune split by 0.03 can therefore be related to a skew quadrupole in a dipole magnet, where $\beta_x \sim \beta_y = 57\text{ m}$ with:

$$\Delta \nu_{\min} = \frac{1}{2\pi} (K_1 L)_{sq} \sqrt{\beta_x \beta_y} \Rightarrow (K_1 L)_{sq} = \frac{2\pi \cdot 0.03}{57\text{ m}} = 0.0033 \frac{1}{\text{m}} \quad (9)$$

The total gradient strength $K_1 L$ is related to the skew quadrupole a_1 in units of the dipole field at injection B_0 with:

$$a_1 = \frac{(K_1 L)_{sq} B \rho_0}{L_{dip} B_0} 10^4 = \frac{0.0033 \frac{1}{\text{m}} \cdot 500\text{ Tm} \cdot 0.0254\text{ m}}{6.12\text{ m} \cdot 0.66\text{ T}} 10^4 = 103 \text{ units} \quad (10)$$

The measured minimum tune split drift is therefore related to a total of ~ 100 units of skew quadrupole in the ring. This is of a similar magnitude as the total amount of normal quadrupole required to explain the tune drift. Distributed over all Tevatron dipoles this corresponds to ~ 0.13 units of $\Delta b_1 / \Delta a_1$. The order of magnitude estimates reveal that relatively weak drifting skew and normal quads can produce the observed coupling and tune drift. Table 1 summarizes the amount of tune and coupling drift in the Tevatron after a 2 hrs injection porch.

Also included in Table 1 is what we refer to as “unexplained” tune and coupling in the Tevatron. The experimentally found tunes in the Tevatron differ from the calculated tunes by ~ 0.16 units [M. Martens, personal communication]. The MAD model of the Tevatron therefore includes a small quadrupolar section that is added to the end of every dipole to match the calculated to the measured tunes. Eqs. (2)-(5) relate this amount of tune to 1.4 units of b_1 in each Tevatron dipole. Similarly a considerable amount of coupling exists in the Tevatron, giving a min tune split of ~ 0.23 units [17]. Eqs. (6)-(10) can be used to relate this minimum tune split to 1.4 units of b_1 in each Tevatron dipole. Most of this coupling has been identified as the a_1 arising in the dipoles as a result of the suspension creep and most of it is now therefore not present anymore in the machine [7,18].

Table 1: Summary of tune and coupling drifts in Tevatron at injection (in units).

	static	dyn (2 hrs)
Tune / b_1 per dipole	0.16 / 1.4	0.015/0.13
Minimum tune split / a_1 per dipole	0.3 / 1.37	0.03/0.13

The reason why the static and dynamic components of tunes and couplings are discussed together will become apparent in the following sections of this report. An important conclusion to be drawn from Table 1 is that the amount of dynamic and static a_1 and b_1 required to explain the tune and coupling drifts as well as the “unexplained” tune and coupling are more or less the same: ~ 0.14 units of dynamic a_1/b_1 (after 2 hrs)

and ~ 1.4 unit of static a_1/b_1 . Also of interest is the 1:10 ratio between the dynamic and static contributions.

3) Summary of a_1 - b_1 Measurements in MTF

The following summarizes extensive measurements conducted at the Technical Division's Magnet Test Facility (MTF) to investigate possible magnet related origins of the tune and coupling drifts. Some of those measurements were performed in the context of the investigation of the suspension creep issue that was identified as the main cause of the strong coupling in the Tevatron. The results of this measurement campaign are summarized in detail in [8]. Those results from this particular study, which have some connection with the issue at hand, will briefly be summarized here. The main purpose of this chapter is to document the search for dynamic a_1/b_1 components in the Tevatron dipoles, a major effort conducted over the last two years at MTF.

Figure 8 shows an example of a skew quadrupole measured in a particular Tevatron dipole (TB0413). This measurement is shown here because it reveals all the features, which will be discussed in the following. First, this magnet obviously has a geometric a_1 of ~ 2.5 units at full field and not zero as it should be according to the Tevatron dipole design. Then, it obviously has a_1 hysteresis, i.e. the excitation and de-excitation branches do not overlap. The hysteresis loop is skewed toward higher a_1 on the ramp, indicating a change of geometric a_1 on the ramp. Finally, the drift (and snapback) effects are clearly visible on the injection and back-porches. Note, however, that this magnet is not typical!

As always with the measurement of very small quadrupolar field in the presence of significant sextupole fields, such as is the case with Tevatron dipole magnets, the possibility of feed-down effects needs to be taken into account. We therefore routinely

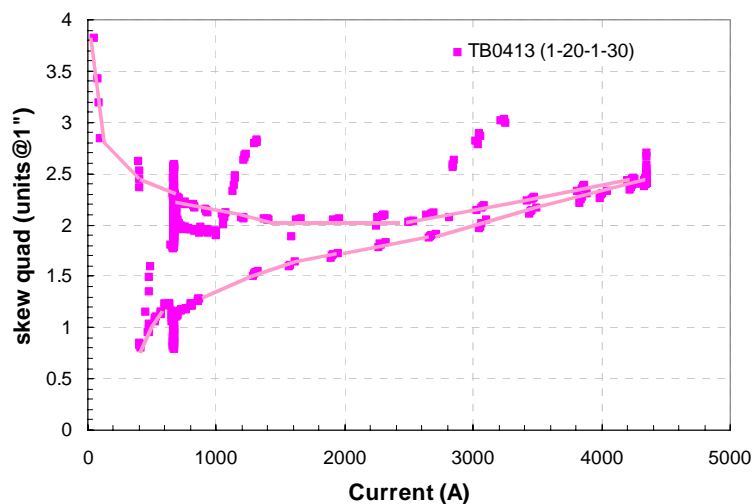


Figure 8: Skew quadrupole in the body of Tevatron dipole TB0413 (measured).

checked if the hysteretic and geometric a_1/b_1 components were consistent with feed-down. That is, if the same systematic geometrical offset of the rotating coil system in the magnet bore, Δy , can explain the observed geometric and hysteretic a_1 taking into account the measured geometric and hysteretic sextupole. If this is the case feed-down from the sextupole is assumed. Such a coincidence was given in only a very few cases, however [11].

3.1) Geometric a_1/b_1

	Combined		
	Ave	σ	No.
b_1	-0.06	0.76	770
a_1	0.01	0.94	770

The table on the left gives the average a_1/b_1 (up-down average at 2 kA) of all Tevatron dipoles manufactured and tested prior to installation. The archived magnetic measurements show that the nominal goal to keep the a_1/b_1 zero (± 1 unit) was achieved.

Note that the effect of the suspension creep, which has caused the a_1 to increase to ~ 1 unit [7], presumably occurred after the original measurements and is therefore not reflected in this table.

Beyond the average content of normal and skew quadrupole, there are some important issues regarding the geometric quadrupole in the dipole. The most important is that the geometric a_1/b_1 components vary across the length of the magnets. In particular in the ends the a_1 can go through a strong spike if the length of the lower and upper poles of the magnets are not equal. Also to be included in this category is the suspension creep effect on the a_1 , which we will also review later in this chapter.

Figure 9 shows the result of a longitudinal scan of the skew quadrupole in Tevatron dipole TC0525. The plot shows the geometric a_1 measured along the axis of magnet 0525 by placing a ~ 1 m long probe in different non-overlapping positions in the magnet. The a_1 variation found is several units (and could still be larger at an even finer scale). The all magnet averages calculated from the data archive are averages over such longitudinal distributions.

We have several explanations for the longitudinal variations of the quadrupole moments in the Tevatron dipoles, mostly related to geometrical coil imperfections. Figure 10 summarizes the major modes of coil deformation. For instance $100\ \mu\text{m} / 50\ \mu\text{m}$ of azimuthal compression of the inner / outer coil of one pole with respect to the other pole introduces 1 unit of a_1 (left sketch in Figure 10). A $2 \times 20\ \mu\text{m} / 2 \times 10\ \mu\text{m}$ of azimuthal

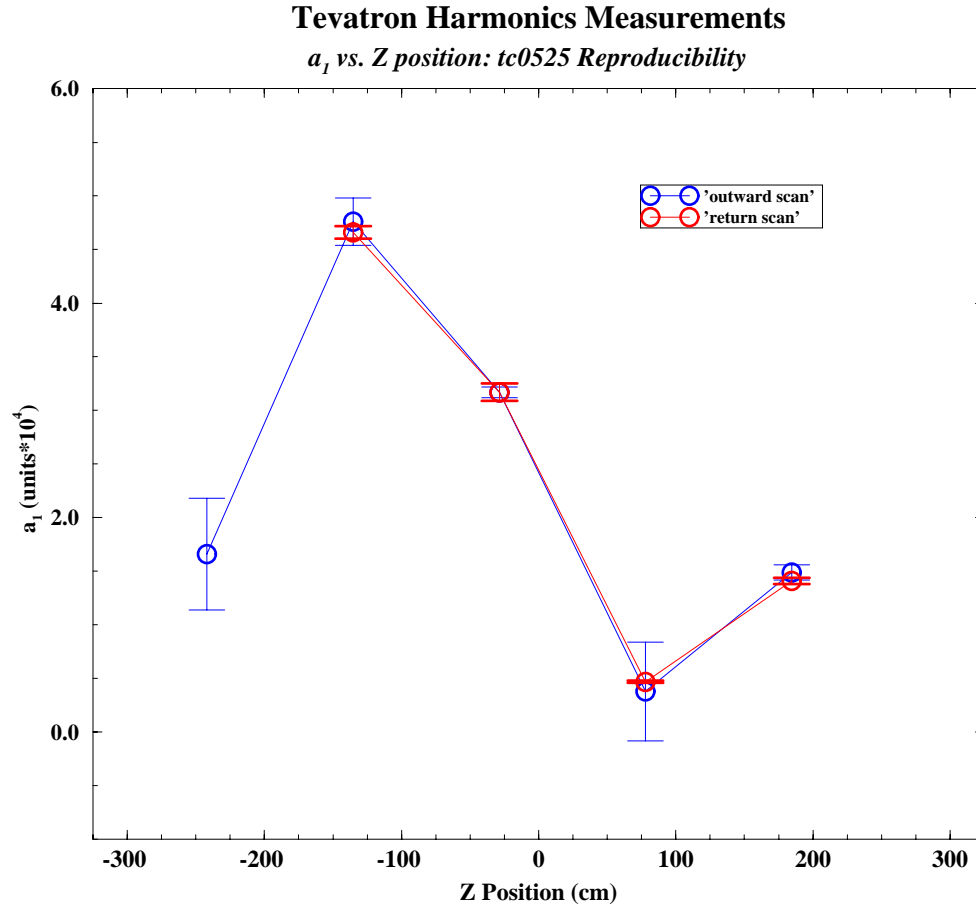


Figure 9: Recent measurement of longitudinal profile of a_1 along Tevatron dipole TC0525. The measurements were obtained with 83 cm long rotating coils. The second measurement was obtained after disassembling and re-assembling the entire measurement system.

compression of one side of the inner/outer coil with respect to the other side introduces 1 unit of b_1 (middle sketch in Figure 10). The right sketch in Figure 10 shows how the coil position relative to the warm iron yoke can vary along the length of the magnet. A $85 \mu\text{m}$ vertical / horizontal de-centering of the coils within the warm iron yoke produces 1 unit of a_1 / b_1 . This, in fact, is the very same iron yoke effect that also produced a_1 in the case of the suspension creep.

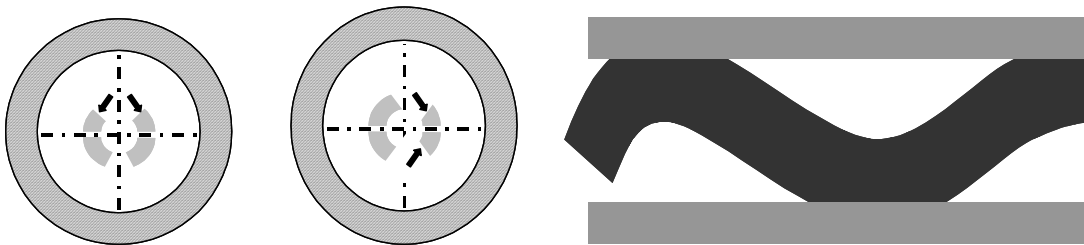


Figure 10: Possible causes for longitudinal a_1 variation along Tevatron dipoles.

Large a_1 excursions in the ends of Tevatron dipoles have been observed. They can be sufficiently large to influence the overall average of the a_1 of a Tevatron dipole and be a leading contributor to the magnet-to-magnet variations of a_1 . There can be an a_1 spike in the ends, if the longitudinal positioning of the ends of the two poles do not perfectly match (a ~ 50 units local excursion of a_1 comes with a 1 mm mismatch). Figure 11 shows a comparison of calculation (1 mm coil length difference) and measurement in TB1055 performed with a 2 cm short rotating coil. Such a 40 unit a_1 excursion in one end couples with 0.5 units into the overall length average a_1 of a Tevatron dipole. Figure 12 shows a_1 measurements in 28 dipoles, in which so-called special position measurements were made in the 1980s (in addition to the standard positions middle & ends, there are two more data sets for intermediate positions). The data are arbitrarily shifted such as to bring the center measurement to zero. The plot clearly reveals larger a_1 variations toward the ends. Note that the measurement points represent the probe centroids of ~ 2.4 m long probes, such as used during the “production” magnetic measurements.

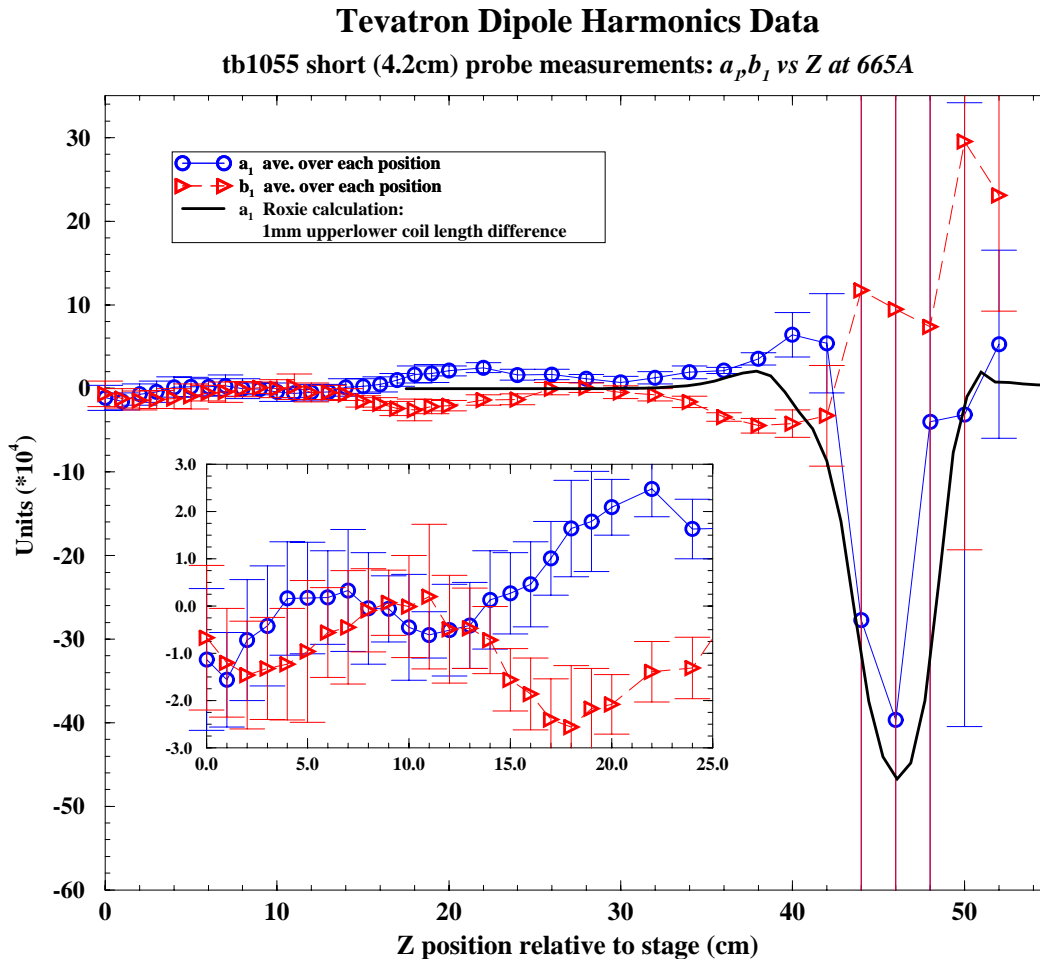


Figure 11: Short probe z-scan in end of TB1055 revealing a strong spike. Also shown: calculation of a_1 for lower and upper pole length mismatch of 1 mm.

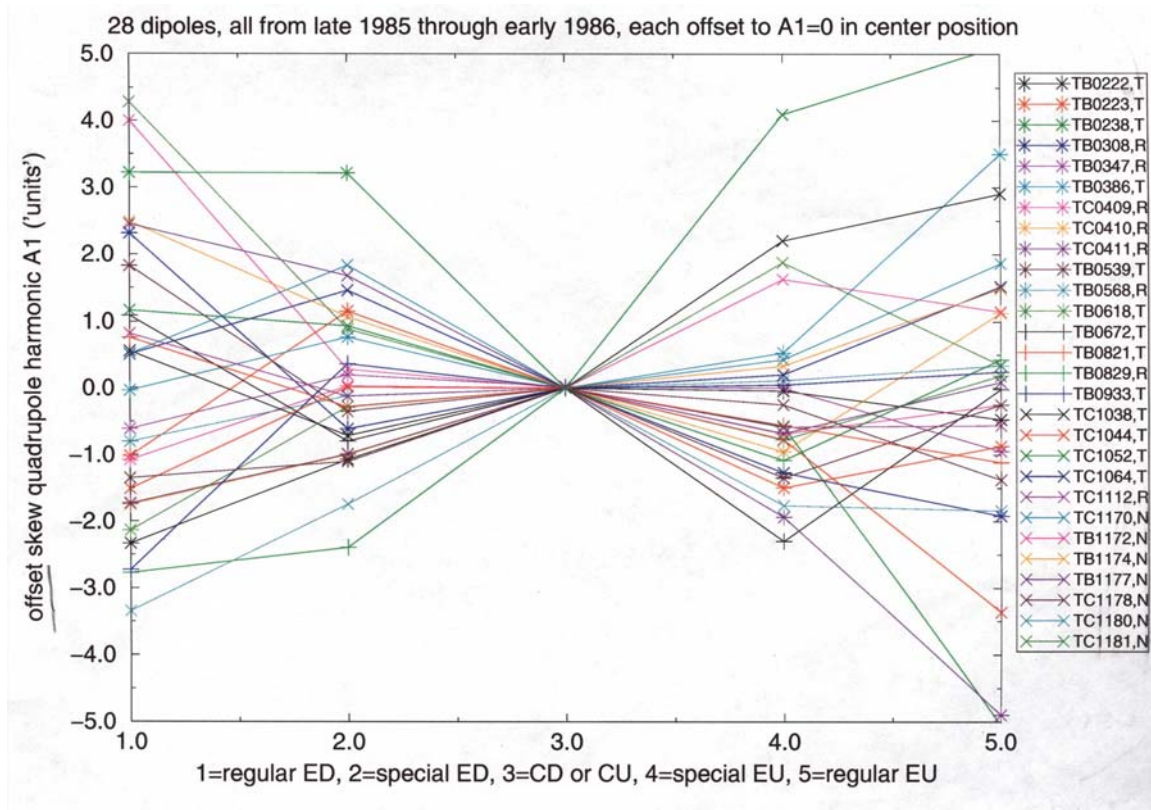


Figure 12: Special measurements were conducted in 28 Tevatron dipoles, in which in addition to the standard measurements, the probes were also placed in intermediate positions. The data series are arbitrarily shifted such that the middle position measurements are zero.

Also mentioned should be the possibility of “measurement” errors in the presence of strong a_1 spikes in the dipole ends. For instance, if the measurement coils are not perfectly concentric in the magnet bore, but canted, strong a_1 due to feed-down from the large b_2 excursion in the ends occurs. Feed-down from the b_2 is usually an important issue in magnetic measurements of a_1 and b_1 (especially in the ends). These issues are discussed in further detail in [8], [11].

As discussed in detail in [7], [8], [18] creep in the Tevatron dipole G11 suspensions caused the Tevatron coils to drop on average ~3 mils within the yoke (as derived from recent and archived “lift” measurements in the installed magnets – the lift is proportional to the distance of the coil from the iron yoke). This introduced an average $a_1 \sim +1$ unit in all dipoles as the result of an up-down imbalance of the iron yoke contribution to the magnetic field in the bore (Figure 13). As discussed in [8] the measurements in MTF have confirmed that this effect had occurred also in the recently tested spare dipoles.

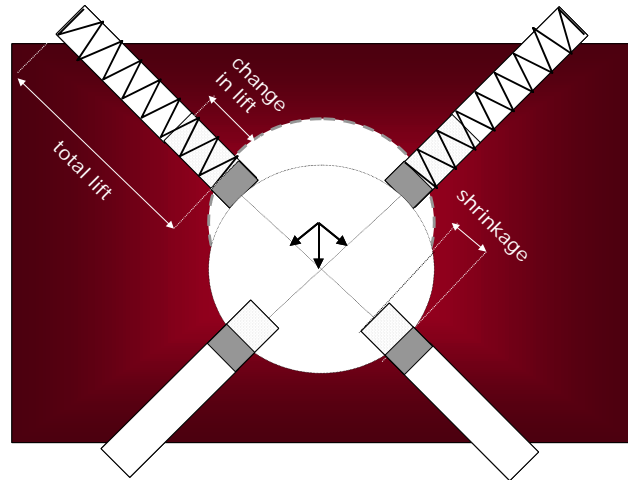


Figure 13: Creep in G11 suspensions caused the coils to drop ~3 mils with respect to warm yoke, introducing a ~+1 unit of a_1 in the Tevatron dipoles.

Summarizing the above said, we have no evidence for any static a_1 / b_1 except for the one unit of a_1 as a result of suspension creep as discussed above. Therefore an additional ~0.4 b_1 and the ~1.4 a_1 units of Table 1 remain to be explained.

3.2) Hysteretic a_1/b_1

As shown in Figure 8 a_1 hysteresis is found in some Tevatron dipoles. The most plausible cause of a_1 hysteresis is that it is the result of differences in the J_c (critical current density) of the superconductor in the upper and lower poles of the dipole magnets. Figure 14 shows the result of a Roxie³ calculation of the a_1 hysteresis in a Tevatron dipole due to this effect. The calculation indicates 1 unit of a_1 hysteresis (at injection) for ~18% of difference in the J_c between upper and lower pole. Note that if the lower pole has higher J_c (and stronger magnetization) the “sense” of the loop is reversed from counter-clock-wise to clock-wise. The J_c values assumed in the calculations vary between 1-1.9 kA/mm² (at 5 T, 4.2 K - in the non copper region), which is consistent with typical variations found in the Tevatron conductors, as is discussed in detail in [9]. The average J_c value in the Tevatron dipoles is ~1500 A/mm² (5 T, 4.2 K). One of the features of the Tevatron conductor development is that improvements in J_c were obtained even during magnet fabrication. Magnets were sometimes assembled from coils made with different batches of superconductor. The late, “hi-ho” material achieved a J_c of ~1800 A/mm².

Note that the up-down J_c differences do not cause a geometric or current dependent a_1 ! Figure 14 also shows a “loop” calculated for the condition with the coils offset in the yoke by +100 microns as occurred on average after the suspension creep. This condition clearly gives only geometric and no significant hysteretic behavior.

³ Magnetic simulation program developed by S. Russenschuck / CERN

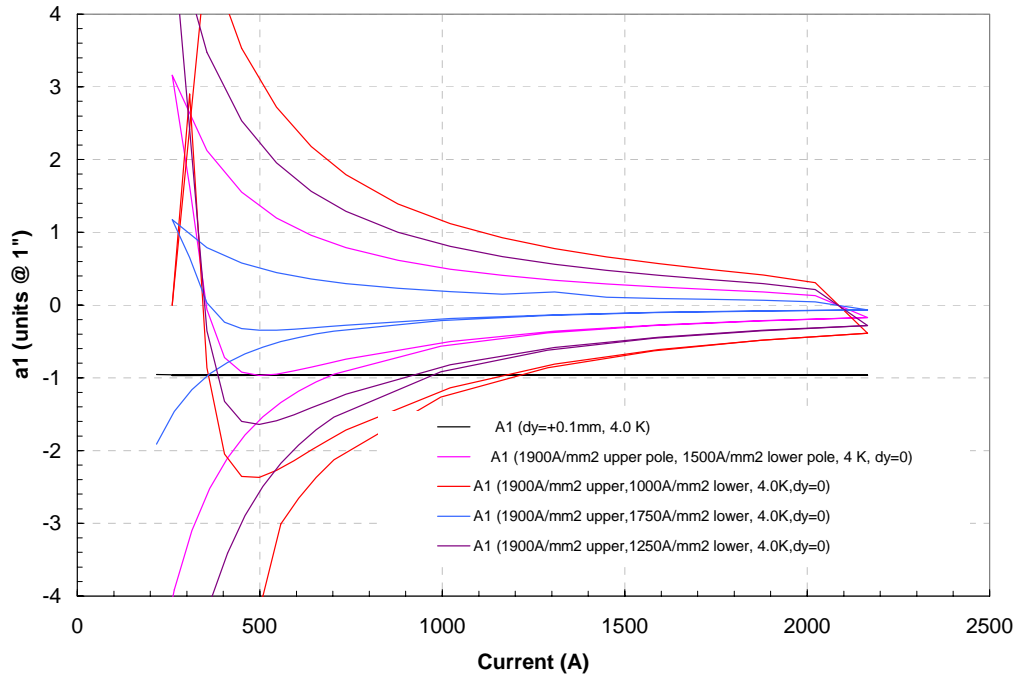


Figure 14: Calculation of a_1 hysteresis with Roxie 9.0 for varying superconductor J_c in lower and upper poles (1000, 1250, 1500, 1750 A/mm², at 5T/ 4.2 K). Also show calculation of effect of cold displacement in yoke, which does not produce any hysteresis.

This model, however, cannot explain b_1 hysteresis, which would require a left-right asymmetry in the conductor properties, an unlikely condition in a dipole magnet. In fact there appears to be no b_1 hysteresis in the Tevatron dipoles. This further strengthens

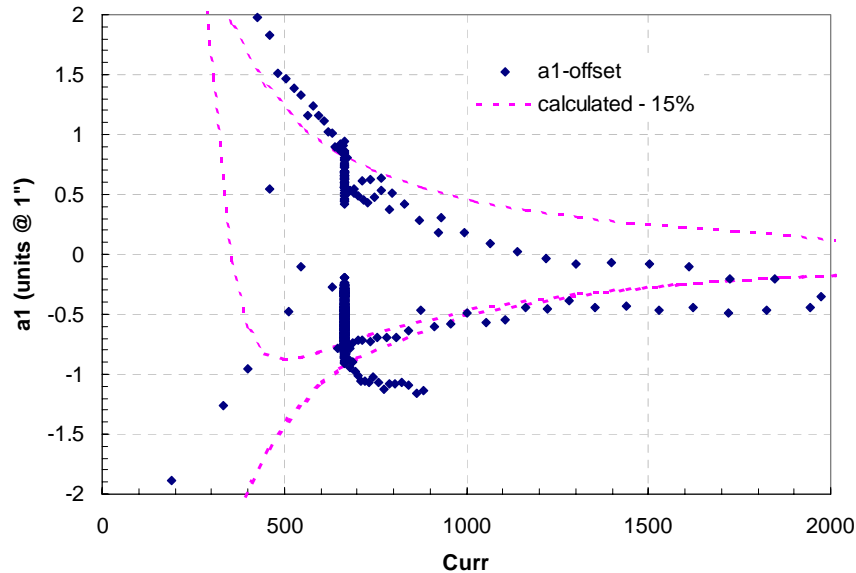


Figure 15: Measured a_1 in a Tevatron dipole as compared to a Roxie calculation assuming a J_c difference between upper and lower pole of 15%.

the case for a_I hysteresis being the result of superconductor J_c differences. Figure 15 shows that an up-down difference of 15% (which is within the expected range of variation) fits the a_I hysteresis measured in a particular Tevatron dipole.

3.3) Change of a_I/b_I on the Ramp

Figure 16 shows the average a_I and b_I of all installed Tevatron dipoles on the ramp from injection to 4 kA. These curves, which were derived from the archived magnetic measurement data, indicate that a_I increases on the ramp. The increase of b_I is less pronounced. Both geometry effects discussed in 3.1) to explain longitudinal variations in a_I and b_I , coil geometry variations and coil de-centering within the yoke, can also depend on the current in the magnet as a result of Lorentz-forces. A change of coupling is observed in the Tevatron during the ramp, consistent with a change of 0.1 units of a_I in the dipoles. Several possible causes will be discussed in the following. They are: hysteresis effects, de-centering forces and coil deformations during ramping.

Note that the a_I curve in Figure 16 does not include the effect of suspension creep, which presumably occurred after these measurements were taken. This effect is expected to shift the a_I curve up by 1 unit and increase the slope up the ramp due to de-centering forces. Also note that drift effects were not considered in the analysis of the archive data (i.e. drifts might have occurred during the fixed current dwells during which the magnetic measurements were taken, but these drifts were not known and hence not recognized)

Figure 17 shows a histogram of the slope of the all-Tevatron average a_I up the ramp (this plot contains exactly the same information as Figure 16. The average slope is very small - 0.05 units/kA, but consistent with an average change of a_I by ~ 0.1 units during the ramp.

The increase of a_I on the ramp could be the result of hysteresis if a large enough number of dipoles would have non-negligible hysteresis. The histograms in Figure 18 show the a_I up-down ramp difference (= hysteresis loop width) at 660 A and 2 kA as derived from the archive data. The distributions are centered on -0.08 & -0.01 units, thus indicating loop widths at least ten times smaller than the a_I loops measured in some magnets (such as shown in Figure 8, for example). This presumably is the result of the fact that many magnets in the population have no hysteretic behavior. It also, however, is the result of mixing of magnets with clock-wise (lower pole has higher J_c) and counter-clock-wise (upper pole has higher J_c) hysteresis loops. In the up-down difference histogram shown in Figure 18, the magnets of the latter variety occupy the side of the distribution toward negative values. The average hysteretic a_I widths derived from the Tevatron archive are therefore too small to be consistent with a 0.1 unit change on the ramp from injection to collision. At best one can assume that the change on the ramp corresponds to the half-width of the average hysteresis, and thus to 0.04 units, less than half of the observed change of a_I on the ramp. Therefore the a_I change on the ramp is probably not only the result of hysteretic effects. Interestingly the average Tevatron

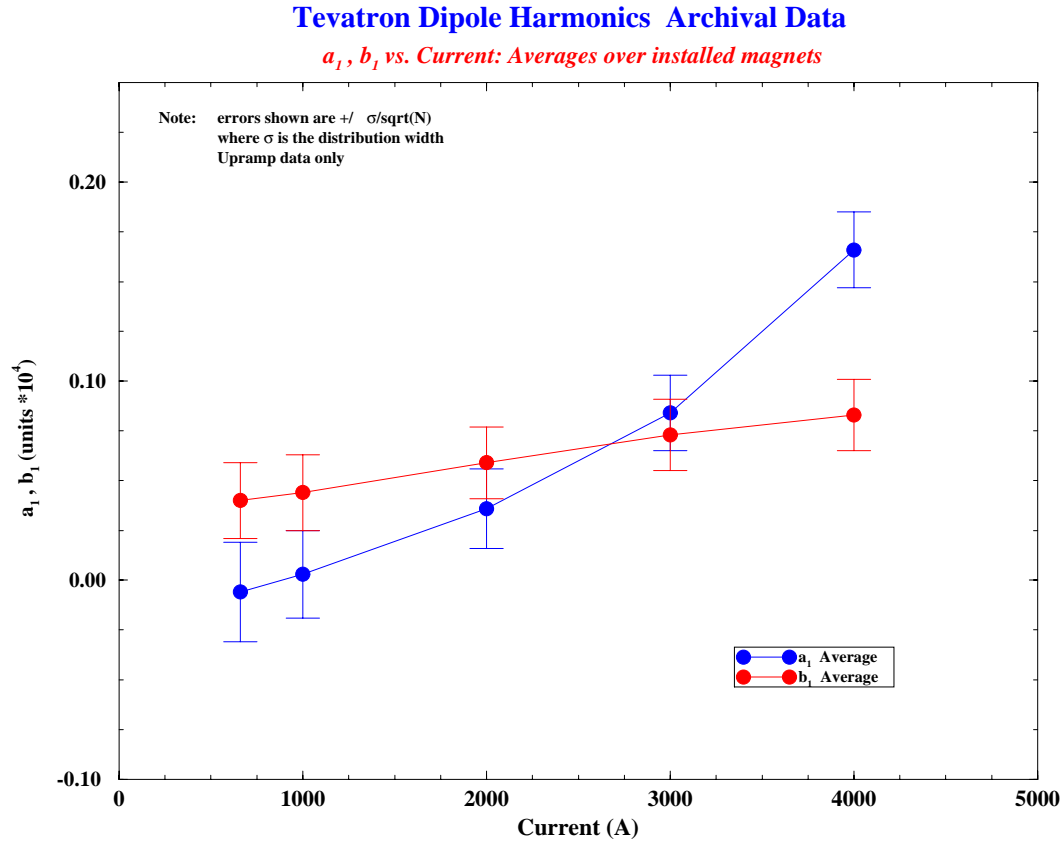


Figure 16: Average a_1 and b_1 of all Tevatron dipoles on the ramp from injection to collision.

08 Jul 2003 13:33:45

File: harmSlpFit_plotFile_1_histFile_01_0307081333.xmgr

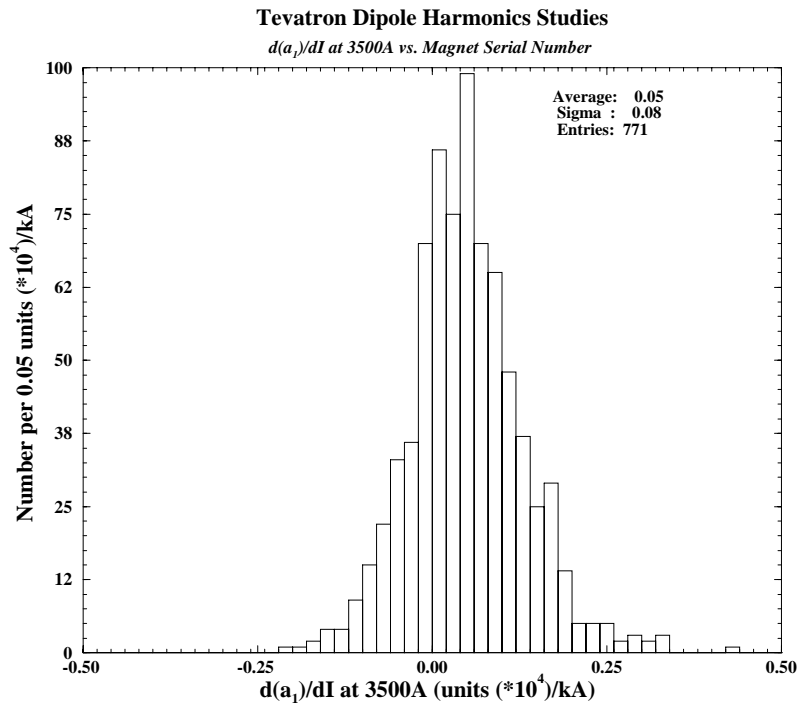


Figure 17: Average slope of a_1 derived from archive data on the ramp.

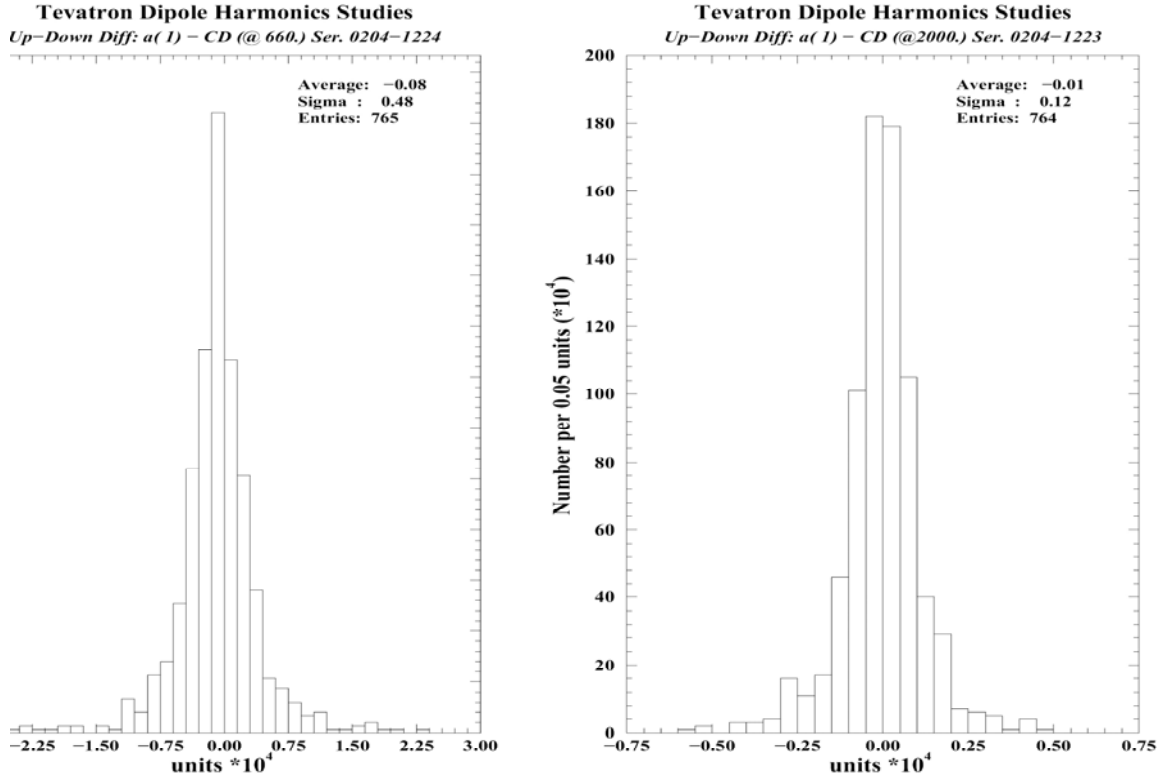


Figure 18: Histograms of a_1 hysteretic width (up minus down ramp) at 0.66 kA and 2 kA.

dipole b_1 does not show a change on the ramp! We also know that there is no b_1 hysteresis. Does this further corroborate that a part of the a_1 change on the ramp must be hysteretic?

Another possible reason for the change of a_1 on the ramp could be the effect of de-centering-forces. If the coils have a systematically built in a_1/b_1 , it is possible that by the re-shimming performed prior to installation in the Tevatron, the coils were actually systematically displaced from the center in order to compensate the intrinsic a_1/b_1 with yoke-effect a_1/b_1 . The systematic coil de-centering within the yoke would lead to de-centering forces on the ramp. Figure 19 shows the calculated de-centering force per support for a Tevatron dipole as function of the coil displacement from center and current in the coils. Strong forces of up to 100 kg per support can be generated for small (order 300 μm) coil displacements. Supports in several Tevatron dipoles were broken during testing in the 1980s after the coils were de-centered by $\sim 500 \mu\text{m}$. This effect was possibly made stronger with the suspension creep. Although the recent discovery of strong coupling in the Tevatron was clearly correlated with the presence of 1 unit of a_1 due to systematically de-centered coils, there is no clear evidence of the effect of de-centering forces. A specially designed experiment in which the coil was displaced by 0.03" to produce de-centering forces showed no effect. This re-shimming experiment is described next.

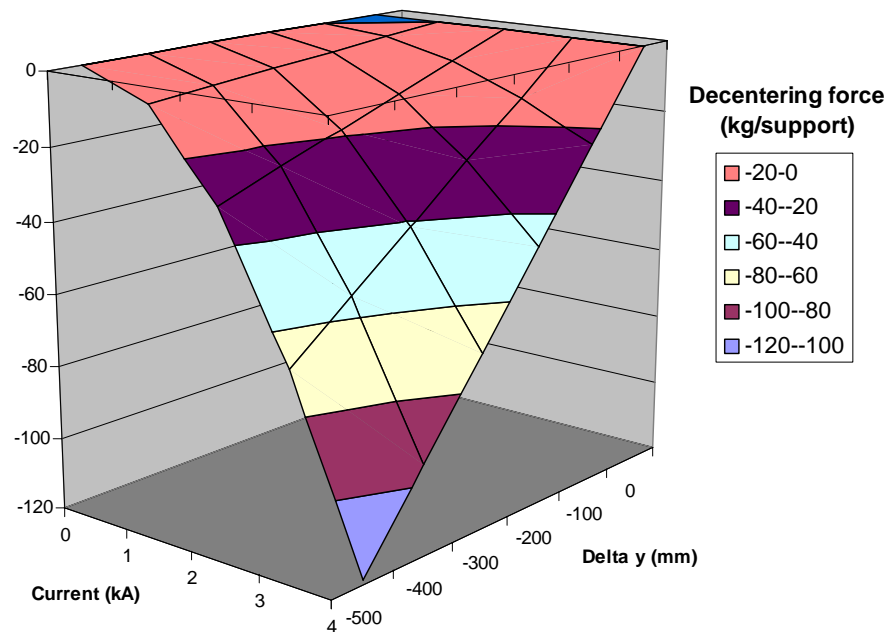


Figure 19: Calculation of the de-centering force (per support) on Tevatron dipole coils as function of coil offset from yoke center and current in coil.

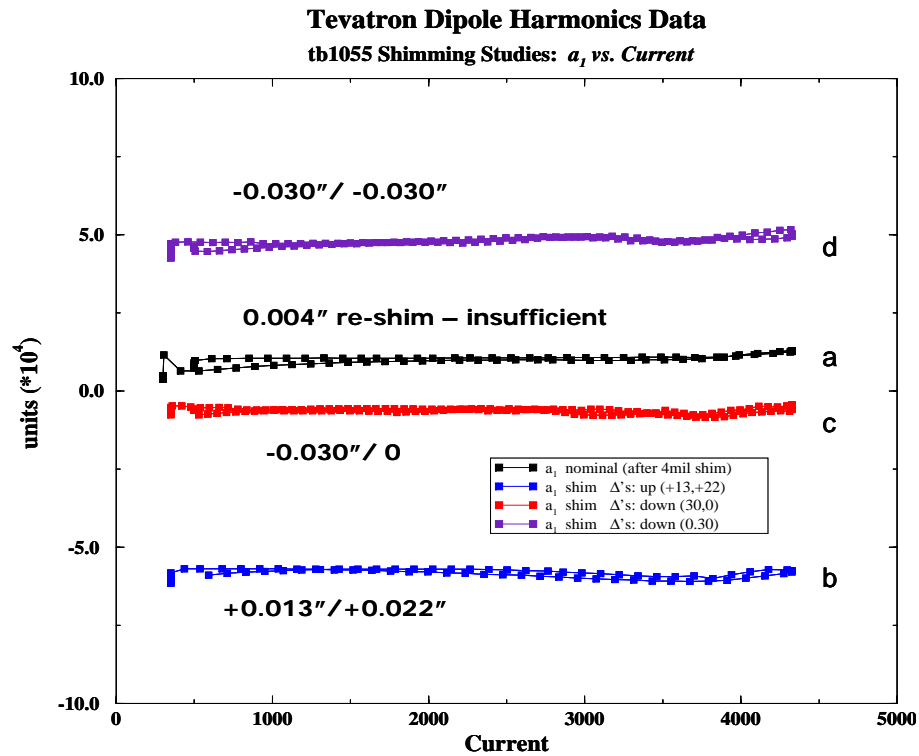
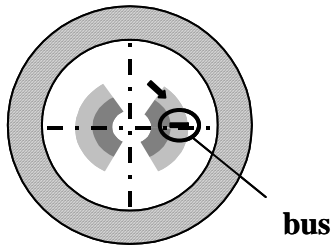


Figure 20: The results of the re-shimming demonstration experiment. The shimming applied in Q1/Q2 is indicated with the curves. Condition b,c, and d resulted in strongly de-centered coils.

Figure 20 shows the results of a shimming demonstration experiment, in which a dipole was re-shimmed strongly (in all suspension stations along its length) such as to bring the coil into extreme off-center positions, horizontally and vertically. Following initial re-shimming ((a), which failed to set a_1/b_1 exactly to zero) the coils were shimmed up to be at 0.015" vertically (b). Then shims were removed from one diagonal to bring the coil to 0.015" horizontally (c). Finally, shims were also removed from the other diagonal, such that the coil ended up at $y=-0.015$ ". As can be seen from the plot the a_1 loops recorded in each case gave the expected change in geometric (6 units at 0.015"). They failed, however, to show a clear signature of a de-centering a_1 .

The third possible explanation for the change of a_1/b_1 on the ramp is coil-deformation on the ramp. The schematic on the left shows one particular mechanism that can explain the appearance of a_1/b_1 changes on the ramp. The Tevatron dipole has the particularity



that the return bus is part of the coil. More precisely the bus forms the outer layer mid-plane turn in the first quadrant. The bus turn has a thick ground insulation (~0.4 mm). In order to keep the symmetry the other three quadrants have symmetrizing shims to make up for the difference in insulation thickness between the bus and a regular turn. If under azimuthal Lorentz-force loading the bus turn compresses by 10% ($=2 \times 40 \mu\text{m}$), ~1 unit of a_1

(0.93) and b_1 (1.153) are produced. The stronger compression moves the outer layer in the first quadrant azimuthally down by 0.1 deg. There are also many other possibilities for non-symmetric coil deformation to produce intrinsic a_1/b_1 and their change on the ramp.

The fact that the all Tevatron average of b_1 shows no change on the ramp is a strong argument against this mechanism. Another strong argument is related to the lack of ramp-dependence in other higher order multipoles. Figure 21 shows the a_2 , a_3 , a_4 and b_3 , b_4 , b_5 multipoles as a function of current on the ramp. Except for b_4 , which is an allowed multipole (decapole) with hysteretic behavior, all higher multipoles do not vary significantly on the ramp as they should if coil deformations would take place.

Summarizing, we believe that we have only partial understanding of the a_1 change on the ramp, namely as partially the result of "residual" a_1 hysteresis. This effect, however, cannot explain more than ~0.04 units of a_1 change on the ramp. Our de-centering force demonstration experiment remains inconclusive. The last possibility for explaining the ramp effect is related to feed-down from the sextupole⁴. The strong evidence for feed-down effects in the Tevatron will be discussed in further detail in chapter 4.

⁴ Feed-down from the sextupole in the dipoles and chromaticity correctors is the result of systematic beam offset in these magnets. Varying vertical and horizontal beam orbits during ramping could explain the change of a_1 and b_1 on the ramp in the feed-down hypothesis.

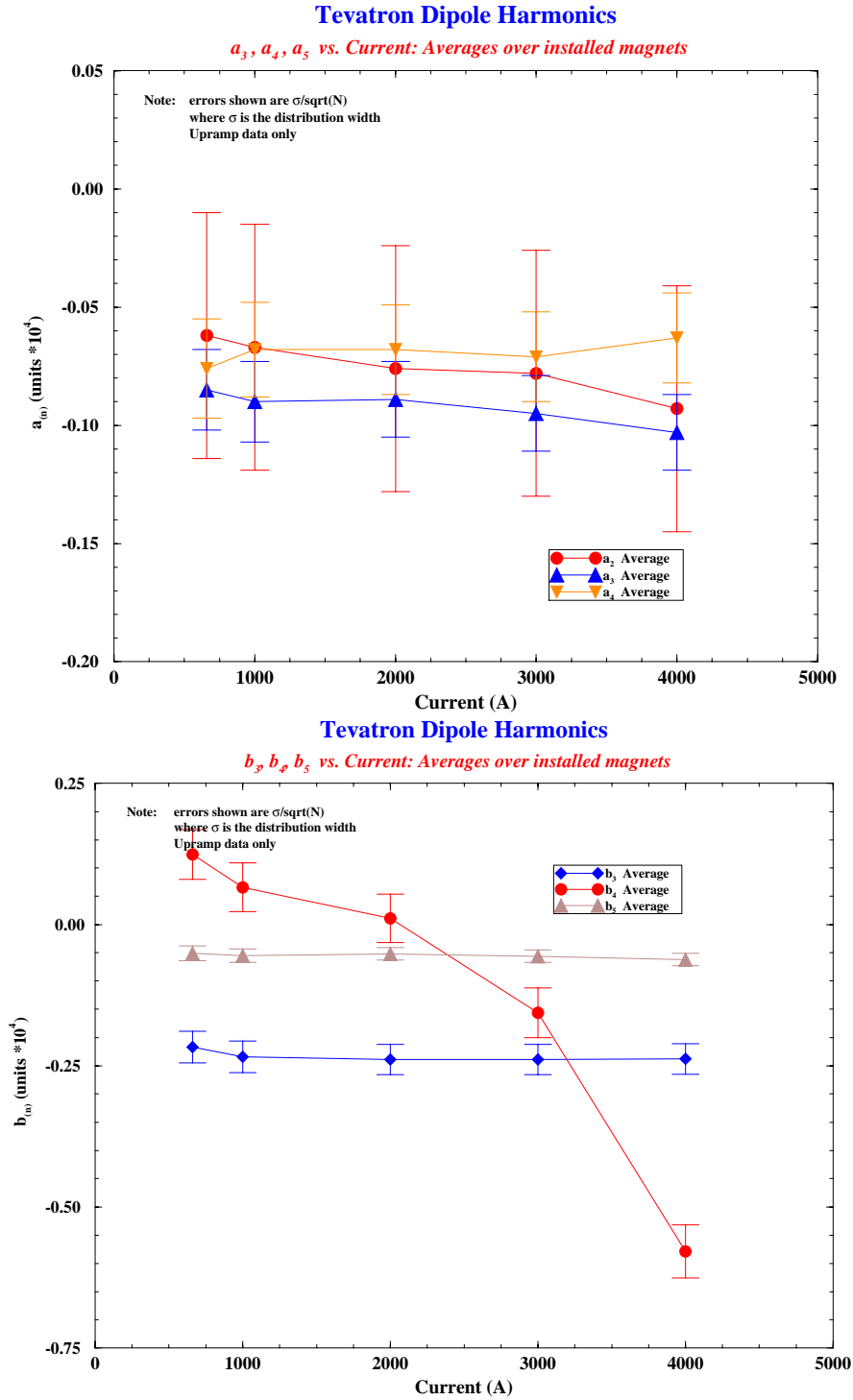


Figure 21: All Tevatron dipole average higher order multipole ramp dependence (from Tevatron magnetic measurement archive).

3.4) Dynamic a_1/b_1 in the Tevatron dipoles

The most straight-forward explanation for the tune and coupling drift in the Tevatron would be intrinsic a_1/b_1 drifts in its main magnets, the dipoles and quadrupoles. The issue of main field drifts in the superconducting main quadrupoles will be discussed in detail in chapter 4.1.). The possibility of intrinsic a_1/b_1 drift in the Tevatron dipoles was investigated extensively during the last two years, since, as shown in Figure 8, some evidence of a_1 drift was found in select Tevatron dipoles. Further details on the measurement technique and particularities of dynamic effects in the superconducting dipole magnets of the Tevatron can be found in [10].

As shown in Figure 22 there is in fact a_1 drift of the order of 0.1 units in many of the magnets tested. This order of magnitude of drift is consistent with the to be explained coupling drift in Table 1. The possible mechanism for a_1 drift is the difference in de-magnetization (the same demagnetization that causes b_2 drift) between lower and upper pole of the dipoles. A difference in de-magnetization can be the result of differences in the dynamics of current (re)distribution (e.g. as a result of different contact resistance or different current distribution patterns) or differences in superconductor magnetization. Figure 22 in fact shows, that the a_1 drift amplitude after 30 mins at the injection porch (following a 1-20-1 min precycle) in a dozen magnets recently measured can be large, but that the signs scatter. As a rule of thumb one can say that if the demagnetization is stronger in the upper pole the a_1 drifts toward more positive values and vice versa. In some cases the sign of the drift reversed after some time. This would be expected if the current re-distribution time constants are different in the lower and upper poles of the dipole. If the signs of the drifts are distributed evenly, the average drift amplitude for the entire machine is close to zero. Unfortunately, given the small sample of magnets tested here, we cannot easily extrapolate to the total ensemble of Tevatron dipoles. Also, we have not studied the history dependence of the drift in detail, such as with the b_2 drift [see 10 for details].

Since the investigated effect is small, the data were carefully checked to exclude feed-down effects from the b_2 -drift. While we have a model to understand a_1 drift, there is no known mechanism that would explain b_1 drift in dipoles. In fact Figure 22 shows that the b_1 drift is at least one order of magnitude smaller, which is close to the sensitivity limit of our magnetic measurement systems. We conclude that it is unlikely that intrinsic $\Delta a_1/\Delta b_1$ drift from the Tevatron dipoles is responsible for the tune and coupling drift in the Tevatron.

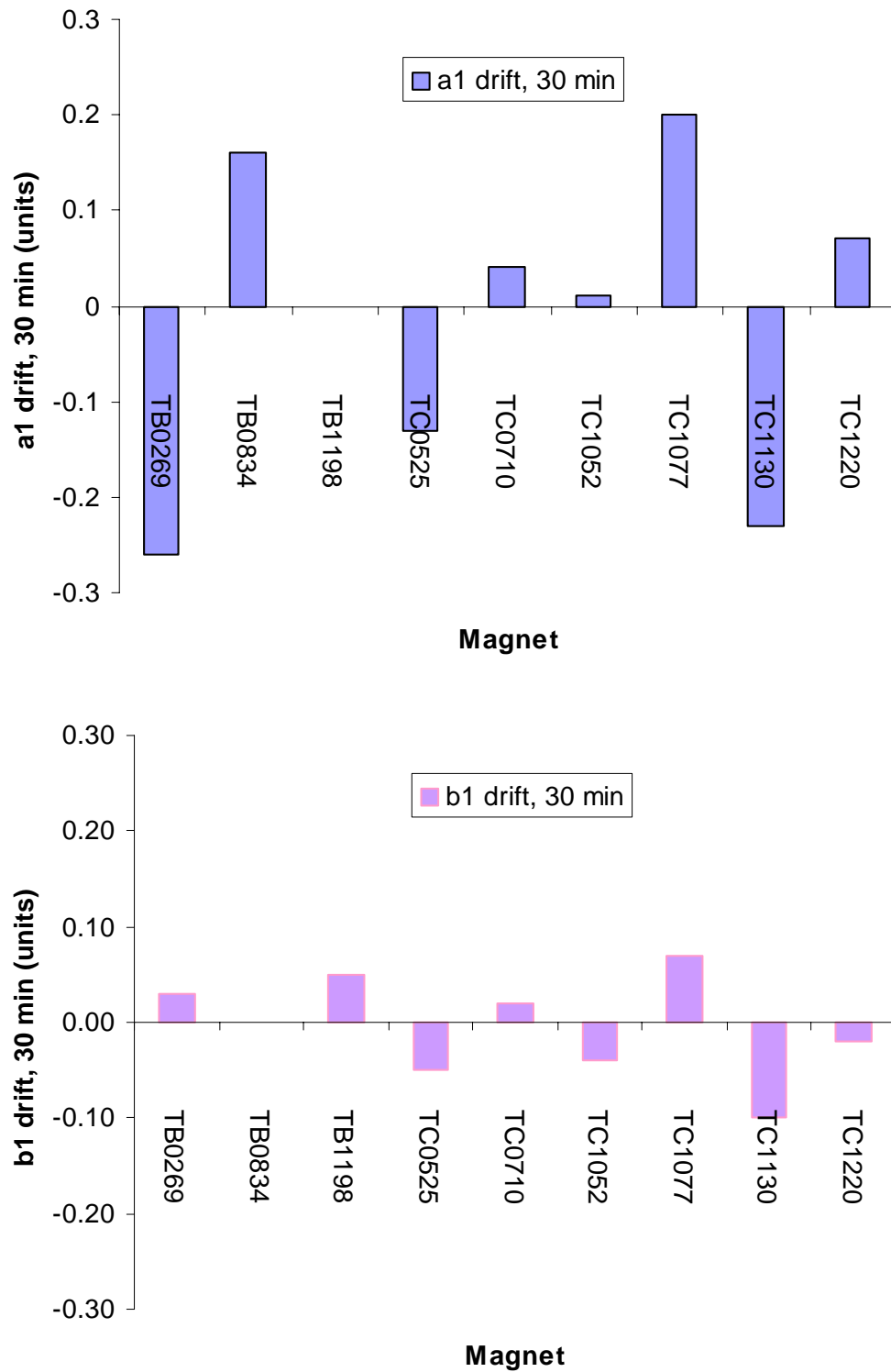


Figure 22: Magnitude of a1 (top) and b1 (bottom) drift after 30 mins on the injection porch (and following a 1 min front-porch, 20 min flat-top, 1 min back-porch pre-cycle) in Tevatron dipoles recently tested.

4) Magnet-based Models for the Tevatron Tune & Coupling Drift

Given the lack of evidence for intrinsic a_1/b_1 drift in the Tevatron dipoles, other magnet based models for the tune and coupling drift in the Tevatron need to be explored. The models also need to explain why the vertical and horizontal tunes drift with opposite signs and why the drift is logarithmic. This chapter will first discuss several possible models that are not feed-down related. Finally we will discuss in detail the models which involve feed-down. The latter are those, which we believe provide us with the most likely explanation of the tune and coupling drift in the Tevatron.

4.1) Non Feed-Down Scenarios

The strong coupling in the Tevatron following the suspension creep which caused the coils to drop on average ~100 microns with respect to the warm magnetic yoke certainly explains a large part of the coupling in the Tevatron. Therefore 1 unit out of the “unexplained” 1.37 units of a_1 per dipole in Table 1, can be explained by this effect alone. The lowering of the coils with respect to the yoke cannot explain coupling drift, however.

Another model that has often been proposed does not withstand further scrutiny: the main field drift in the superconducting main quadrupoles of the Tevatron. Experimental evidence discussed in [12] indicates that the main field drift in the main dipoles of the Tevatron is approximately 1 unit. This drift is the result of the same processes as those responsible for the b_2 drift. If the main field in the dipoles is drifting we have to expect that the main field in the quadrupoles also drift during the injection porch. Indeed there is recent experimental evidence for main field drift in the Tevatron quadrupoles [13]. Two units (of 10^{-4} of the main dipole) of drift in the main field of the 280 Tevatron quadrupoles can explain the observed horizontal tune drift. This drift is typically toward a stronger focusing field and this is consistent with the reduction of the horizontal tune during the drift. It cannot, however, explain the drift with opposite sign of the vertical tune, indicating an increase in de-focusing in the vertical plane. There is no reason to assume that the main field drift should be toward weaker fields in the vertically focusing quadrupoles.

One more element needs to be mentioned when discussing main field drift in quads. Equ. 11 shows that equal (relative) drift in the dipoles and quads result in no change of the tune ΔQ . The increased horizontal focusing in the horizontally focusing quads is exactly balanced by the increase in dipole field, which, in conjunction with the phase-focusing in the accelerating RF cavities, result in a larger equilibrium beam energy, offsetting exactly the increase in focusing strength in the arc quadrupoles.

$$\Delta Q = \xi_{nat} (\Delta b_0 - \Delta b_1) \times 10^{-4} \quad (11)$$

Finally, as discussed in [14], systematically inward roll was found during the start of run II in the Tevatron magnets. The systematic component of the roll can explain coupling due to an a_l component appearing in the rolled quads $\sin\phi b_l$. With the b_l drift being of the order of units, the a_l drift expected from the roll is completely negligible. The roll of the main dipole magnets, however, can contribute to the coupling drift, however, in a different, indirect way, as will be discussed next in the context of feed-down related models.

Also to be mentioned here are measurements that were performed to eliminate the low-beta quadrupoles as possible sources of the problem. Due to the large β these magnets have much larger effects on the beam than regular lattice quadrupoles. In this special experiment [15], the low beta quads were not ramped during the (beam-less) pre-cycle, thus causing a drastic change in the “powering history” of the low-beta quadrupoles. Subsequent measurements of the tune drift did not reveal any measurable changes in the pattern.

Finally, the possibility that a quadrupole corrector could accidentally have been wired into the sextupole corrector circuit, was proposed. Since $\sim 6.75 A$ are needed in a standard quadrupole corrector to compensate for the tune drift, and the sextupole correctors typically operate with $1 A$ or less to compensate for the b_2 change in the main dipoles, six or even seven quadrupole correctors would have to be “accidentally” wired into the sextupole circuit. This appears unlikely, especially since three independent checks were performed during installation to prevent just this from happening (visual inspection, voltage drop on leads, field leakage).

4.2) Basics on Static and Dynamic b_2 in Tevatron Dipoles

The feed-down models, which will be discussed next, use feed-down from the b_2 in the Tevatron dipoles (and b_2 -correctors) as a result of systematic horizontal and vertical beam offsets, to explain the tune and coupling drift in the Tevatron. In the feed-down model tune and coupling drift naturally derive from the b_2 drift in the Tevatron dipoles. Before going into the details of the various feed-down scenarios, the basic features of the static and dynamic b_2 in the Tevatron dipoles need to be introduced.

Figure 23 shows our best estimate of the static b_2 profile along the average Tevatron dipole magnet. The longitudinal profile clearly shows the negative b_2 spike in the ends. Also worked into this profile is the fact that the all Tevatron average geometric b_2 is 1.2 units (i.e. the integral over the profile gives this value). Finally the hysteretic b_2 at injection is also included such that the total integral over the profile would result in a total of -4.5 units of b_2 . The b_2 pattern was not taken into account because its period is a few inches, much less than β .

Figure 24 shows a similar profile for the longitudinal distribution of dynamic b_2 . The profile is normalized and needs multiplication with the actual amount of Δb_2 drift (units).

Analysis of Possible Magnet Related Causes of Tune and Coupling Drift in the Tevatron

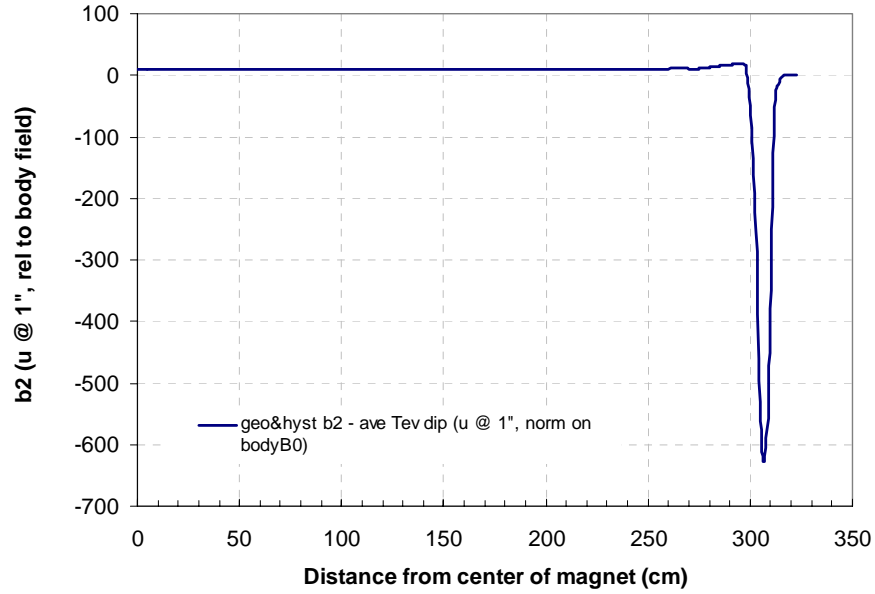


Figure 23: Static (=geometric + hysteretic) b_2 profile in units along the average Tevatron dipole magnet.

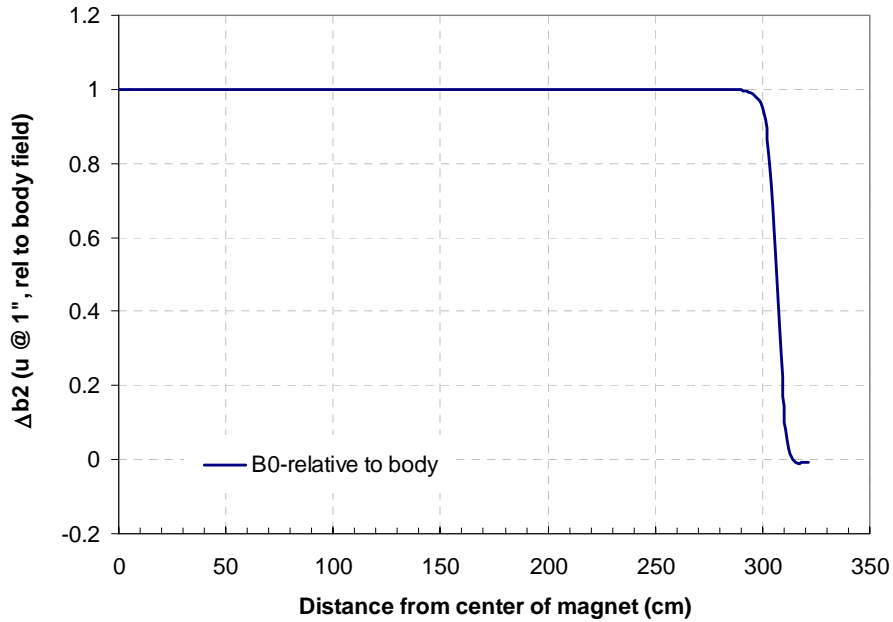


Figure 24: Dynamic Δb_2 profile in units along the average Tevatron dipole magnet. Note that the profile is normalized to one and needs to be multiplied with the actual Δb_2 drift to become meaningful.

The drift profile essentially shows that the drift amplitude is constant along the length of the magnet and that it winds down in the ends in the same way as the main dipole field.

This characteristic is consistent with b_2 measurements recently conducted in several Tevatron dipoles [10].

The feed-down scenarios evolve around the various contributions to systematic beam-offset. The following will develop various beam-offset scenarios and via integration over the length of the average Tevatron dipole magnet the average feed-down effect from the static and dynamic b_2 will be obtained. Note that the basic feed-down effect can be calculated with Equ 12:

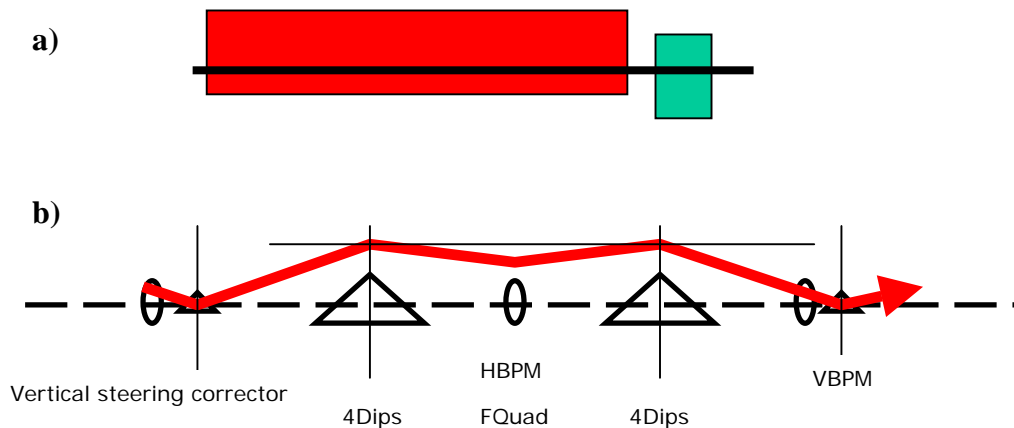
$$a_1 = 2b_2 \frac{\Delta y}{R_0}, \quad b_1 = 2b_2 \frac{\Delta x}{R_0} \quad (12)$$

Equ. 12 translates a 1 mm systematic beam offset into ~ 0.35 units of static a_1/b_1 (for a total average b_2 of -4.5 units) and ~ 0.15 units of dynamic $\Delta a_1/\Delta b_1$ (for a Δb_2 drift of 2 units).

4.3) Feed-Down Scenarios: a) constant beam offset

If the beam is systematically offset horizontally/vertically from the central axis of the dipole magnets, b_1/a_1 feed-down is generated according to Equ. 12. Note that the corrector sextupoles in the spool-pieces next to the quadrupoles inject a b_2 that compensates for the static and dynamic b_2 components in the dipoles⁵. A constant offset in both the dipoles and sextupole correctors therefore produces no net feed-down to b_1/a_1 . It is therefore crucial for the constant offset scenarios that the average beam offset from center is different in the dipoles and sextupole correctors.

The two schematics below represent two likely scenarios producing a net feed-down effect from the b_2 in the dipole magnets. Scenario a) is that of a systematic difference in beam offset between the dipole magnets and sextupole correctors. Scenario b) describes the so-called scallop orbit, which arose in the Tevatron as a result of the systematic roll of



⁵ Note that the fact that the chromaticity correctors also supply a compensation for ~ 20 units of natural chromaticity and ~ 5 units of set-point chromaticity was not included in the above calculations.

the dipole magnets producing vertical deflection of the beam. These two scenarios will be discussed in detail in the following.

To obtain a total of *100 units* of b_1 drift as a result of feed-down from the *2 units* of Δb_2 drift (over ~ 100 min) in the 774 main dipoles, an average, systematic dipole displacement x of:

$$\Delta b_1 = 2N\Delta b_2 \frac{x}{r_0} \Rightarrow x = \frac{100 \cdot 0.0254}{2 \cdot 2 \cdot 774} = 0.84 \text{ mm} \quad (13)$$

is required. A similar, systematic vertical beam offset Δy produces the *100 units* of a_1 drift observed in the Tevatron as coupling drift during injection.

BPM data shown in (Figure 25, Figure 27) from [1,2] indicate an average horizontal / vertical displacement of the beam from nominal of -0.4 mm (radially inwards, consistent with a $-1.1 \cdot 10^{-4}$ relative momentum error) / ~ 0 mm [1]. It is not clear how the BPM readings are related to the actual position of the beam in the dipoles. If the BPM data are correlated with or representative of the average beam offset in the dipoles, the claim could be made, that almost half of the observed tune drift is the result of feed-down from the decaying sextupole fields in the main dipoles as a result of systematic mis-steering. It is more complicated, however, because the same systematic beam offset in the sextupole correctors would produce feed-down that exactly cancels that from the dipoles. It is therefore rather the difference in systematic orbit offset between horizontal orbits in the

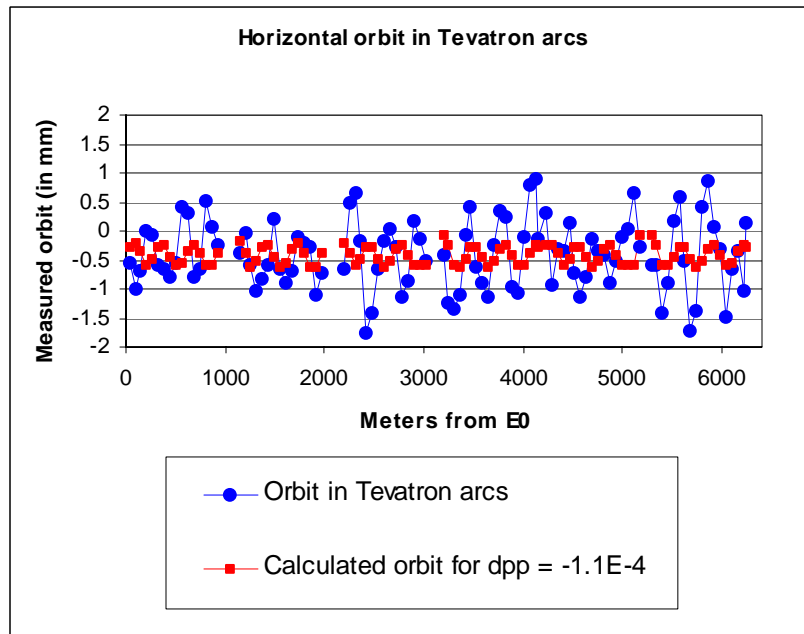


Figure 25: Horizontal BPM readings for Tevatron beam in “center-orbit”. The readings are consistent with a orbit calculation assuming a momentum offset from nominal $\Delta p/p = -1.1 \cdot 10^{-4}$, which in turn is consistent with a systematic beam offset of ~ 0.4 mm (radially inwards).

dipoles and sextupole correctors that counts. Beam-based measurements performed in May 2002, described next, give an indication of the average beam position in the sextupole correctors.

The tunes of the Tevatron were measured as a function of time at 150 GeV, as a function of RF frequency, and current in the T:SF and T:SD sextupole corrector circuits. The data were collected on 5/15/02, [2], while the Tevatron was at 150 GeV after a 30 minutes store at 980 GeV. At each RF frequency offset (-40 Hz, -20 Hz, 0 Hz, +20 Hz, +40 Hz) the tune was measured with 1) no change in T:SF and T:SD, 2) +0.5 Amps added to T:SD, and 3) +0.5 Amps added to T:SF. To be independent of tune drift the measurement was performed after waiting 60 minutes at injection field. The result of the measurements shown in Figure 26 indicates, that on average the beam is aligned with the sextupole centers at an additional $\Delta f \sim 20$ Hz for the case of the T:SD family and $\Delta f \sim 0$ Hz for the T:SF family. Via the slip-factor this can be related to a relative momentum change of $\sim 1.5 \cdot 10^{-4}$. The negative momentum change reflects the shorter circumference orbit that is required for consistency with the increase in RF frequency. This change indicates that the standard orbit is, on average, displaced by +0.34 mm in the T:SD sextupoles. The data suggests that the average orbit offset in the T:SD sextupoles is +0.34 mm horizontally and the average orbit offset in the T:SF sextupoles is -.03 mm although the vertical tune and horizontal tune measurements for T:SF give different average orbit offsets. (No attempt was made to estimate the errors on these measurements.)

The schematic below summarizes the two types of horizontal beam offset measurements discussed above. An average 0.4 mm radial inward displacement of the beam (as derived from the BPM data) together with a 0.34 mm radially outward

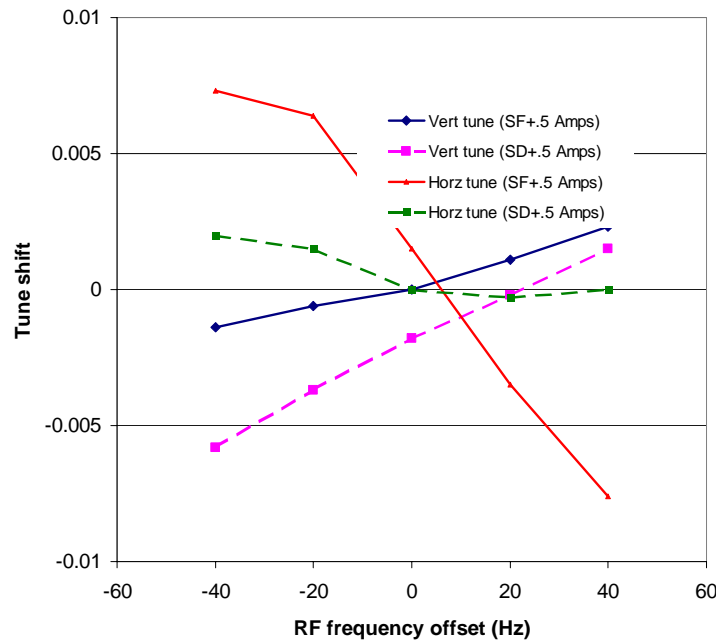
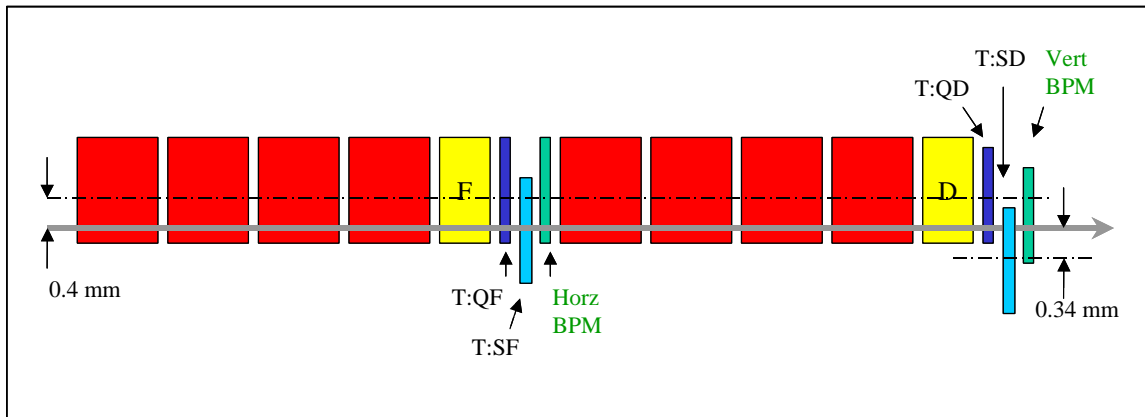


Figure 26: Tune shift from change in T:SF and T:SD as function of RF frequency offset from nominal (after 60 minutes at 150 GeV).



displacement of the T:SD sextupole corrector family (as derived from the orbit variation studies) would indeed produce part of the “unexplained” tune (0.16 units, as given in Table 1). This hypothesis obviously assumes that the horizontal BPMs are aligned with the dipoles (which is actually not a likely situation).

The skew quadrupole could be generated by a similar displacement scenario for the vertical direction. Figure 27, however, shows that 2002 vertical BPM data give no indication of any significant, systematic vertical beam offset. An effect, which does not exist in the horizontal plane, however, can explain a systematic vertical beam offset and the centering in the BPM. A systematic dipole roll (measured to be inwards in the case of the Tevatron – [14]) introduces vertical bending. A simple calculation (Equ. (14)), based on a roll of $\Delta\phi=8$ mrad, measured in some Tevatron dipoles, reveals a large effect.

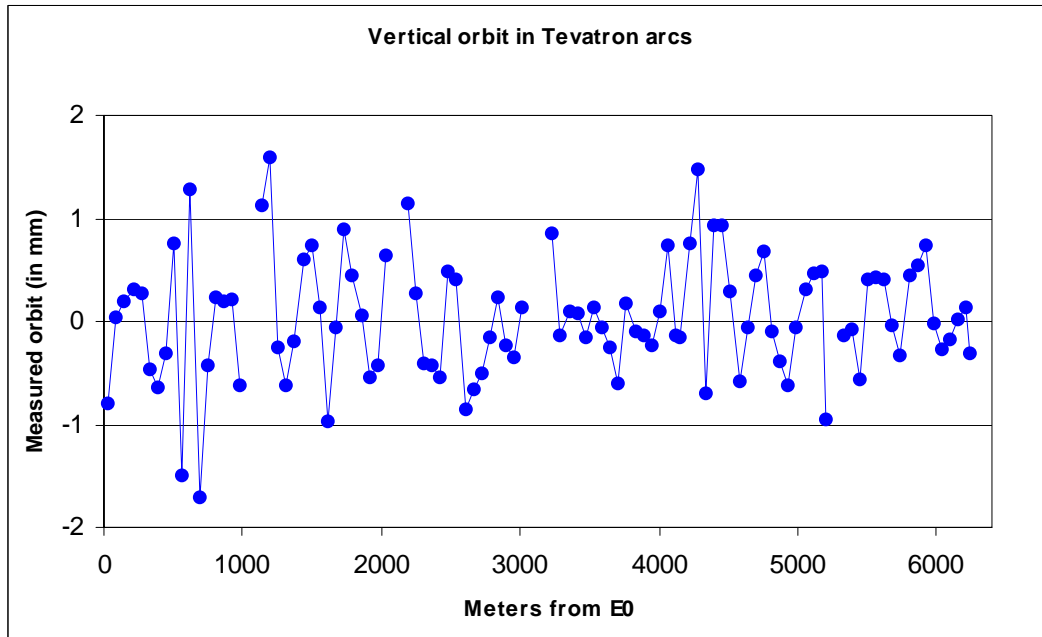


Figure 27: Vertical BPM readings do not indicate any systematic beam offset.

Given that each dipole bends the beam velocity vector by $\Psi=8$ mrad and that there are 8 dipoles (and 60 m) between each vertically focusing quadrupole, a possible maximum vertical displacement of $\Delta y=30$ mm would ensue. Even if the average roll is much smaller, there is still enough vertical displacement left for skew quad feed-down. Most importantly, however, the steering correction used to minimize the vertical beam offset in the vertical BPMs does not remove the systematic vertical beam offset within the cell.

$$\Delta y = \Psi_{mag} \Delta \phi N_{mag} L = 8 \text{ mrad} \times 8 \text{ mrad} \times 8 \times 60 \text{ m} = 30 \text{ mm} \quad (14)$$

Figure 28 shows the integral of the roll angle along the Tevatron ^[16]. As shown in the plot a 1.4 mrad systematic roll of the dipoles in 42% of the ring produces the same total integrated roll. Syphers has shown in [14] that a 1.4 mrad roll in a cell produces an average vertical beam offset due to the scallop orbit of 0.6 mm. The above estimate for the integral, systematic roll of the arc quadrupoles therefore translates into a ~ 0.3 mm systematic vertical offset over the entire ring, which in turn gives ~ 0.1 units of static a_1 (for a total average b_2 of -4.5 units) and ~ 0.05 units of dynamic a_1 (for a b_2 drift of 2 units).

The exact amount of beam offset in the dipoles, quadrupoles and sextupole correctors will remain unknown for some more time (until the Tevatron BPM and magnet alignment system upgrades are complete). What can be said today, however, is that there is ample evidence for systematic 0.1 - 1 mm order beam offset in various Tevatron components. This order of magnitude offset is, as was shown above, sufficient to explain most of the tune and coupling drift in the Tevatron by feed-down. Summarizing, we find on the basis of select direct and indirect measurements of the beam offset in the Tevatron dipoles, that

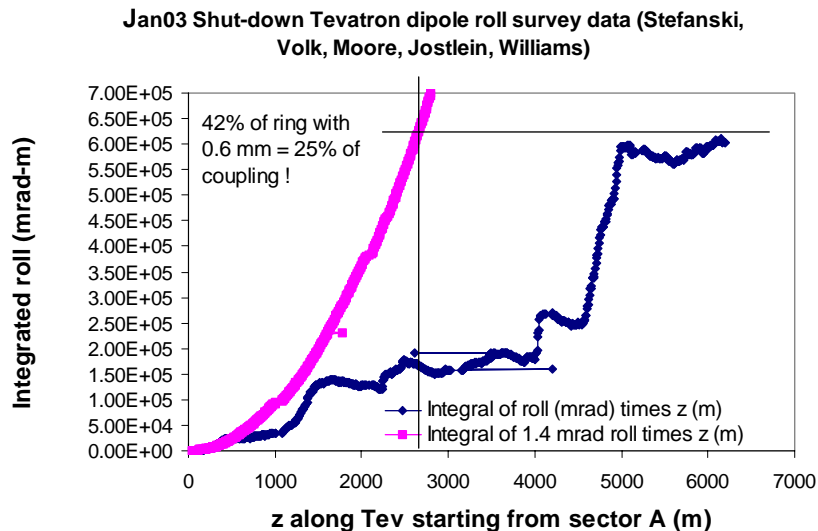


Figure 28: Integral of the dipole magnet roll measured in the Tevatron by Joestlein and Volk during the January 2003 shutdown.

the fixed offset scenarios explain:

- 1) $\sim 20\%$ of the “unexplained” tune / coupling ($\sim 0.2 / \sim 0.1$ units of static b_1/a_1)
- 2) $\sim 50\%$ of the observed tune / coupling drift ($\sim 0.075 / \sim 0.05$ units of dynamic b_1/a_1)

as a result of feed-down (Equ. 12) from the average static and dynamic b_2 profiles in the Tevatron dipole magnets (Figure 23 and Figure 24).

4.3) Feed-Down Scenarios: b) variable beam offset

The schematics below show possible geometrical modes that produce feed-down from b_2 to a_1/b_1 due to variable beam offset within the magnets. Systematic horizontal beam offset from the center of the magnet axis can occur when the magnet sagitta is systematically different from the design value (~ 6 mm) or as a result of yaw. Systematic vertical beam offset can be the result of systematic dipole sag and tilt. The effects can be quantified using Equ. 12 and the b_2 profiles in Figure 23 and Figure 24. The b_2 drift amplitude assumed in the calculations is 2 units. The results are summarized in Table 2. The following discusses these calculations in further detail. The discussion will also clarify the meaning of the benchmark numbers given in the table to quantify the various geometrical modes.

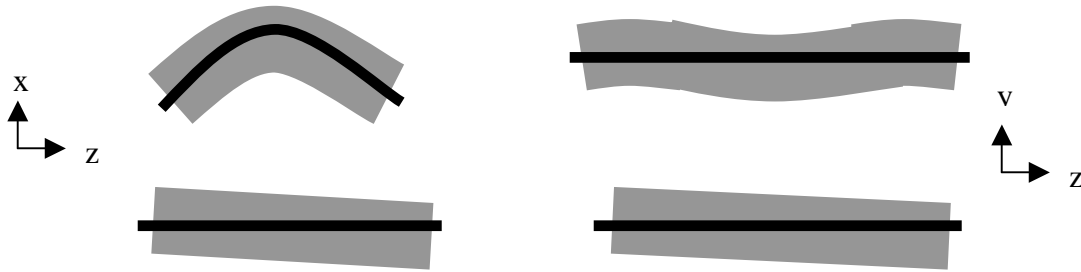


Table 2: a_1/b_1 feed-down from b_2 in variable beam offset scenarios. b_2 profiles as given in Figure 23 and Figure 24 (2 units of b_2 drift assumed).

1 mm sagitta (energy) error	$b_1=+1$ u, $\Delta b_1=0$ u
1 mm magnet yaw	$b_1=+0.2$ u, $\Delta b_1=-0.05$ u
1 mm magnet sag	$a_1=-1$ u, $\Delta a_1=-0.2$ u
1 mm magnet tilt	$a_1=+0.2$ u, $\Delta a_1=-0.05$ u

Assuming a systematic sagitta error in the dipoles magnets as shown in Figure 29 and the b_2 profiles in Figure 23 and Figure 24 one obtains the feed-down profiles shown in Figure 30 and Figure 31. The sagitta error function is symmetric with respect to the magnet center. As becomes clear in Figure 29 the magnet sagitta is assumed to be less pronounced than the beam sagitta, such that the beam runs on the outside of the magnet axis in the middle of the magnet and on the inside from the magnet center line in the

ends. As becomes clear in Figure 30 this particular beam offset produces a strong feed-down to b_1 in the magnet ends where the static sextupole in the magnets is very pronounced. A different sagitta error profile (i.e. not symmetric with respect to the

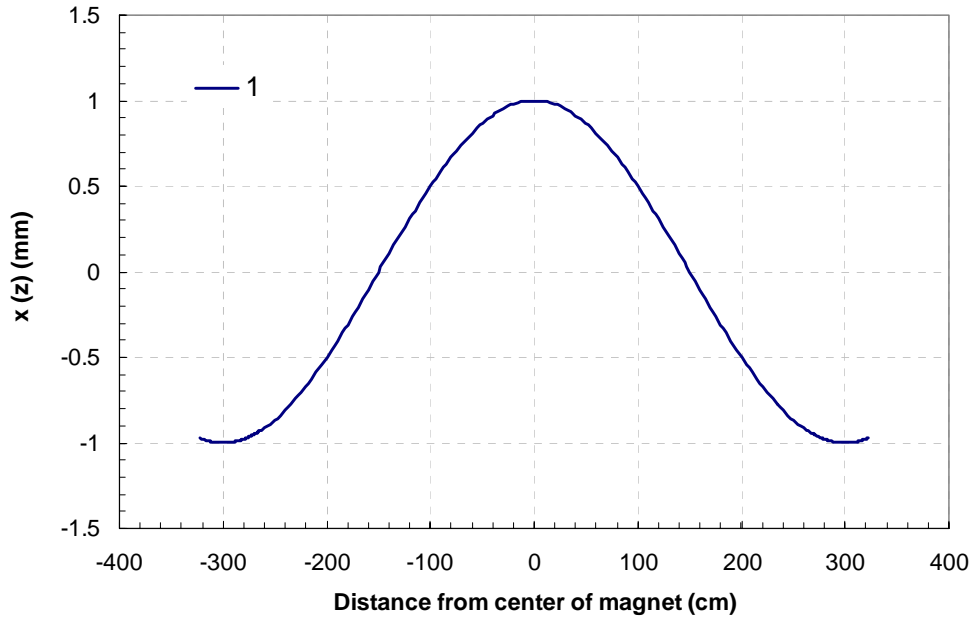


Figure 29: Sagitta error, i.e. difference between beam sagitta and magnet center axis. It is assumed there are two crossover points between the beam trajectory and the magnet center axis, half-way between the magnet center and the ends.

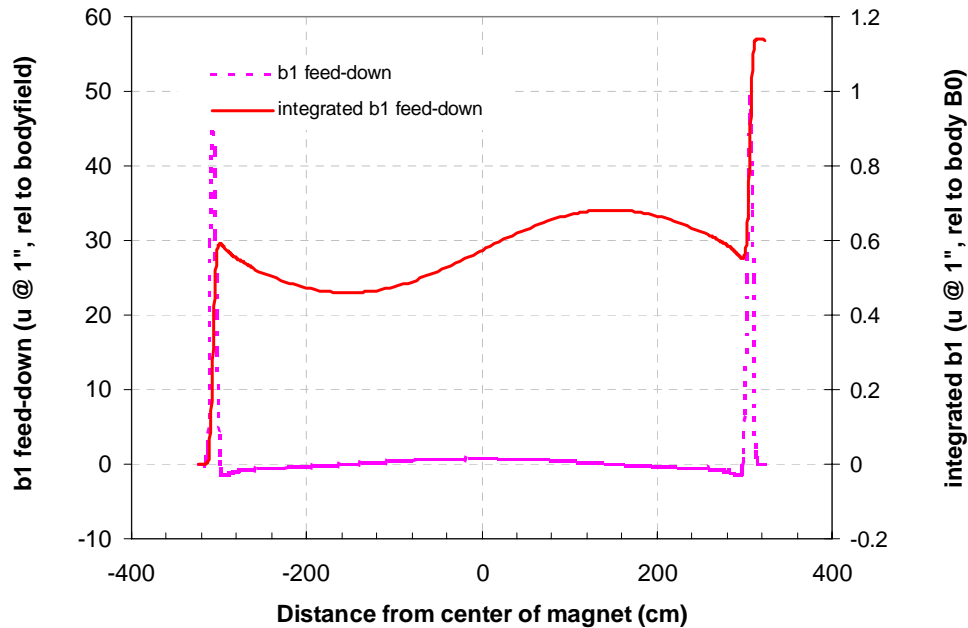


Figure 30: Feed-down calculation for the b_2 profile in Figure 23 and the geometry function in Figure 29.

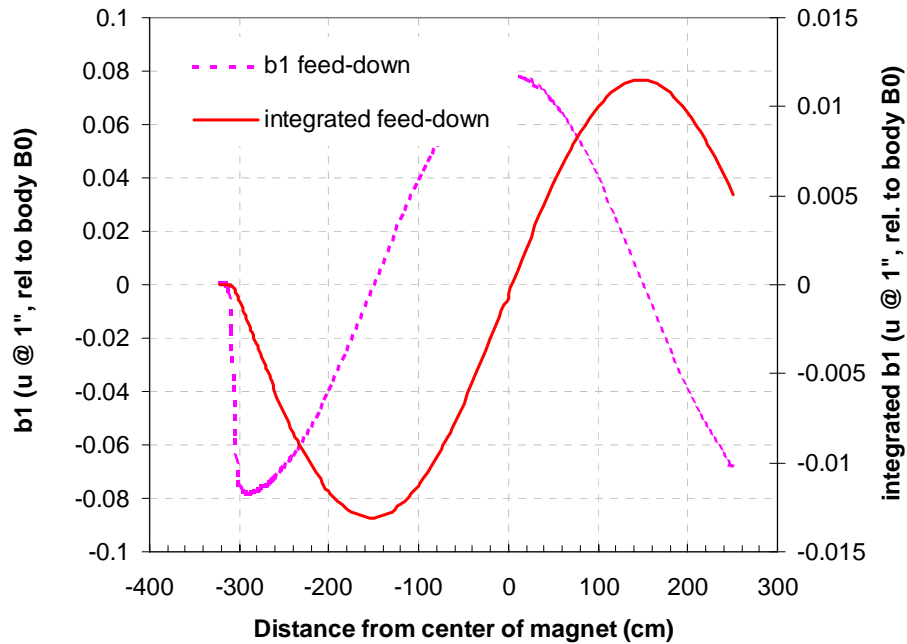


Figure 31: Feed-down calculation for the b_2 profile in Figure 24 and the geometry function in Figure 29.

middle of the magnet) would certainly also reduce the feed-down in the ends. On the other hand the particular geometrical profile chosen produces hardly any feed-down to the dynamic db_1 (because there is not much dynamic b_2 in the ends!). This particular feed-down scenario therefore explains strong geometric and weak dynamic feed-down. As discussed in section 2), the static and dynamic $b_1/\delta b_1$ in the Tevatron that we attempt to explain have a 10:1 ratio.

Assuming a systematic yaw of the dipoles magnets as shown in Figure 32 and the b_2 profiles in Figure 23 and Figure 24 one obtains the feed-down profiles shown in Figure 33 and Figure 34. The yaw function is not symmetric with respect to the magnet center and completely arbitrary. In fact this particular function was chosen because it represents a worst-case scenario. In this case the feed-down from the static b_2 is strongly mitigated because the body-end compensation of the b_2 is almost fully activated. Since such compensation does not exist in the case of the dynamic b_2 the feed-down to the dynamic Δb_1 is fairly strong. Therefore this particular scenario can explain a situation in which there is more dynamic than static feed-down.

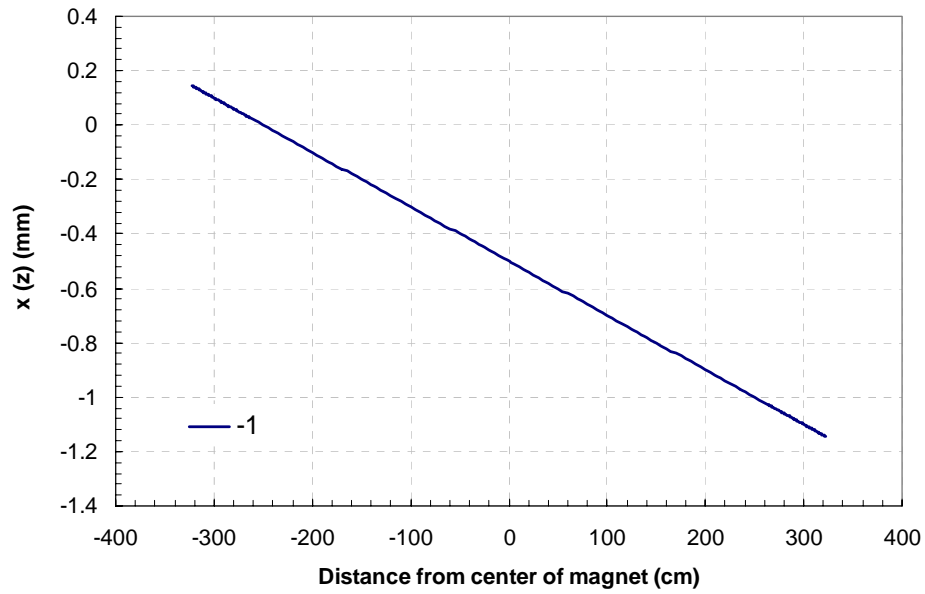


Figure 32: Deviation of the beam trajectory from the magnet center axis as a result of magnet yaw. It is assumed that the beam is centered in one point close to the left side end.

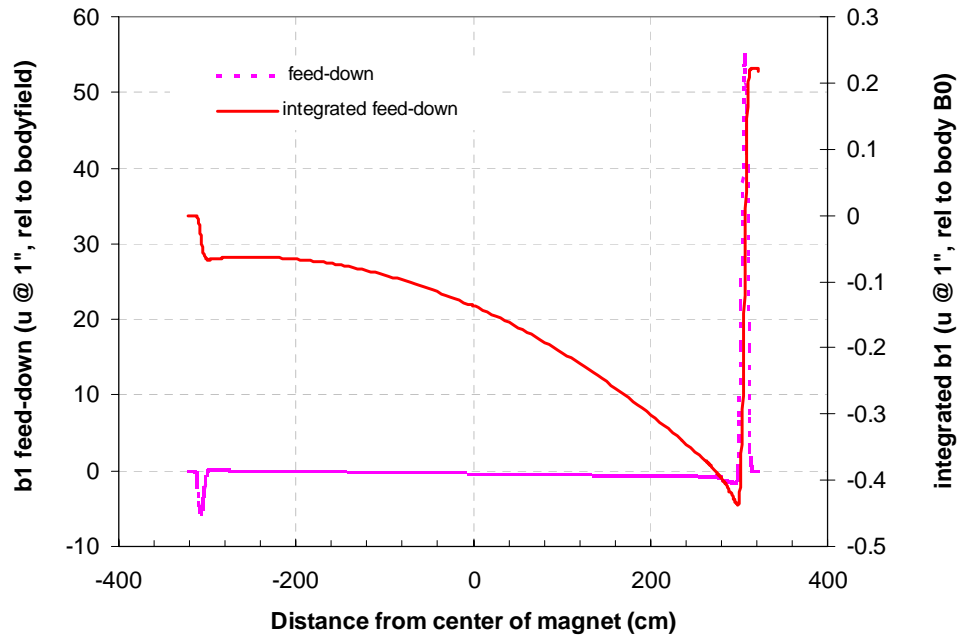


Figure 33: Feed-down calculation for the b2 profile in Figure 23 and the geometry function in Figure 32.

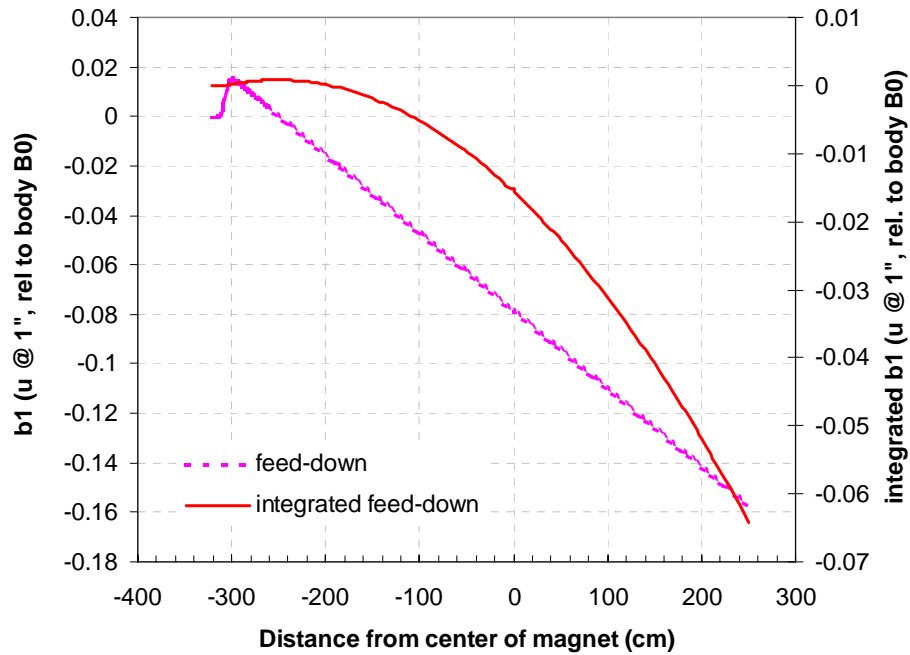


Figure 34: Feed-down calculation for the b_2 profile in Figure 24 and the geometry function in Figure 32.

The beam-offset profile in Figure 35 shows an “invented” magnet sag condition in which the beam is centered in the magnet in the support points and above/below the magnet axis in the middle/ends. Two different gravitational sag-profiles are shown, characterized by a 0.5 mm and a 1 mm maximum excursion in the middle of the magnet. Note that the magnets are interconnected into a string in the ends. The profile in Figure 35 attempted to take this into account. Figure 38 shows survey results obtained by T. Sager’s team on three Tevatron dipoles revealing shape-functions that are very similar to the profile in Figure 35.

The feed-down calculations show that sag produces both strong feed-down to a_1 and Δa_1 . The former is caused by the fact that the shape function changes sign at the support such that the body end compensation of the geometric b_2 is “short-circuited”. The latter is caused by the significant integral beam offset in the magnet body.

Vertical magnet tilt produces a similar amount of feed-down to a_1 as magnet yaw produces $b_1/\Delta b_1$.

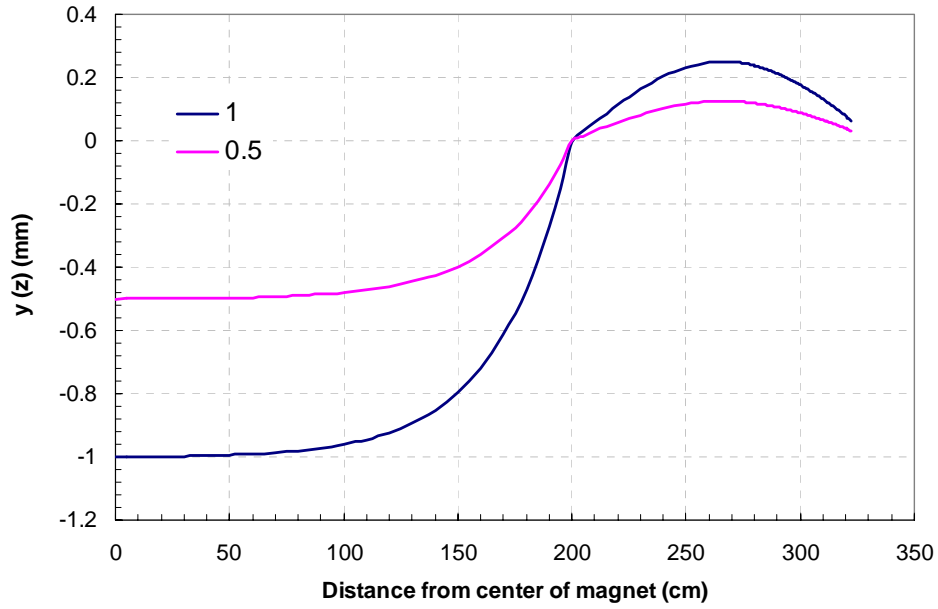


Figure 35: Beam-offset produced by magnet sag. The beam is centered in the magnet in the support points and above/below the magnet axis in the middle/ends.

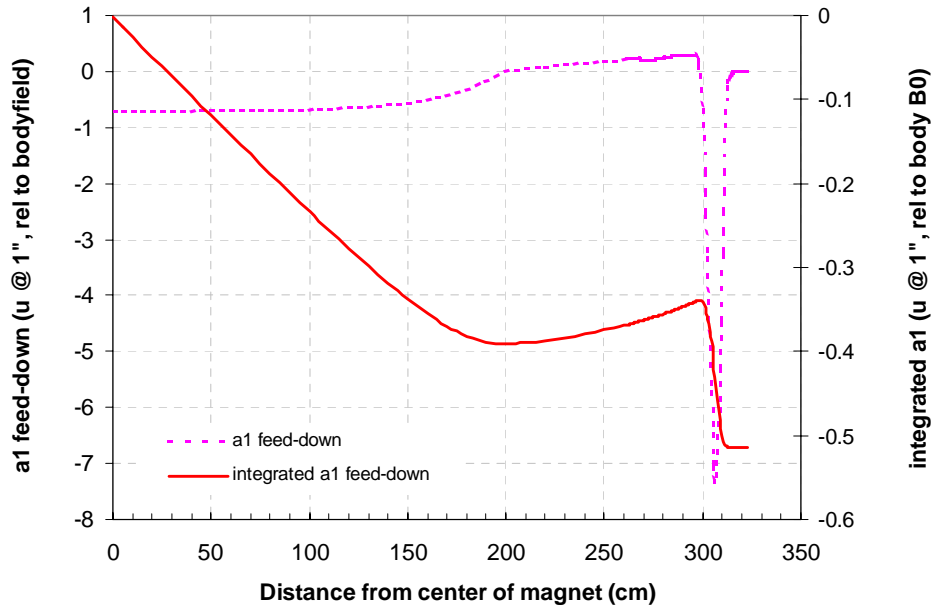


Figure 36: Feed-down calculation for the b2 profile in Figure 23 and the geometry function in Figure 35.

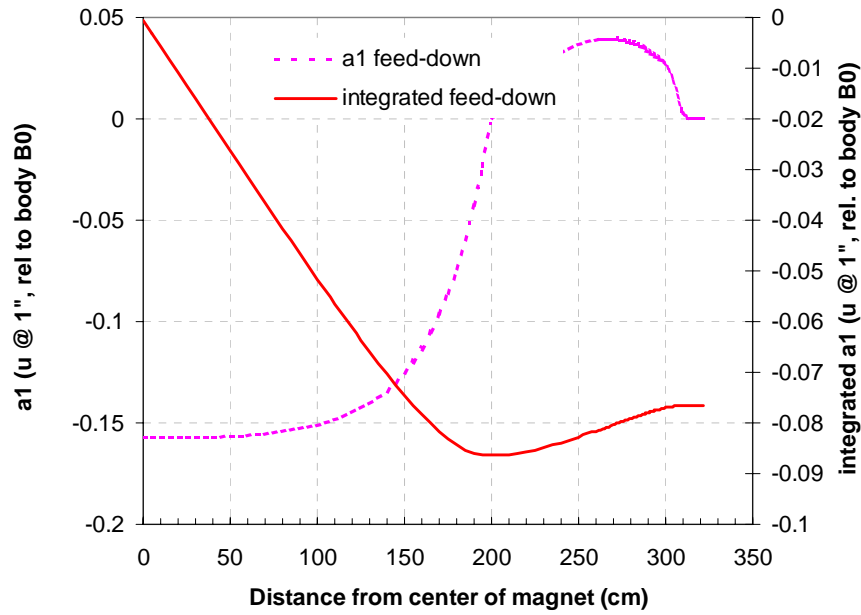


Figure 37: Feed-down calculation for the b2 profile in Figure 24 and the geometry function in Figure 35.

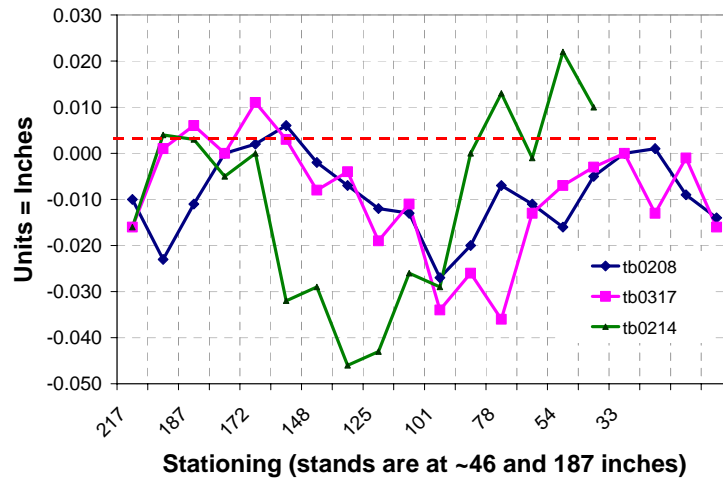


Figure 38: Vertical survey results obtained on several Tevatron dipoles in MTF.

5) Summary

This report discusses in detail the issue of possible magnet related causes of tune and coupling drift in the Tevatron. Following an introduction in which the experimental findings in the Tevatron are summarized, the report discusses in detail our knowledge of the small, residual quadrupole components in the main superconducting magnets of the Tevatron. Although counter-intuitive, we found that the source of the effects is most likely not in the quadrupole magnets (main or correctors) themselves. Therefore most of the emphasis is on the dipole magnets. The analysis of the tune and coupling drift leads us to the conclusion that the most likely explanation for the above described effects is feed-down: Beam offset in the main dipoles and/or sextupole correctors result in skew and normal quadrupole fields due to feed-down from the sextupole fields. The strength of the feed-down scenario lies in the facts that it naturally explains -1- the logarithmic decay and snapback and -2- the fact that the vertical and horizontal tunes drift by a similar magnitude but with opposite sign. Furthermore feed-down also elegantly explains tune and coupling components in the Tevatron, which could not be explained before. Chapter 4 of the report has shown that (directly or indirectly) measured geometrical modes of systematic beam offset of the order of 0.1-1 mm in the Tevatron main and corrector magnets suffice to produce the sought amount of feed-down.

An important part of the experimental work discussed here is the search we conducted for intrinsic skew and normal quadrupole fields within the main dipoles. This effort was not trivial given the minuteness of the quadrupolar fields causing the tune and coupling drifts in the Tevatron (assuming the effect is distributed over all main magnets in the ring). We found very little evidence for significant a_1/b_1 in the Tevatron dipoles, except for the one unit of a_1 that appeared in them following installation in the ring as a result of creep in their G11 suspensions. This effect, however, has been amply discussed and is further described in many documents. It is also being corrected for by a ring-wide magnet re-shimming campaign currently under way. Although we found drift in the skew quadrupole in some dipole magnets (with random signs), we believe that there is no evidence for systematic dynamic $\Delta a_1/\Delta b_1$ in the superconducting Tevatron dipoles.

An important aspect of the feed-down scenarios is that they explain unaccounted tune and strong coupling at the same time. It has been a mystery for many years why artificial quadrupolar fields needed to be added to the Tevatron lattice models to explain the experimentally observed tunes. Strong coupling in the Tevatron was recently discovered to be mostly the result of the suspension creep, but some additional coupling beyond that is present in the machine. The feed-down hypothesis naturally explains these effects as feed-down from the static (geometric and hysteretic) components of the sextupole fields in the Tevatron dipoles and chromaticity correctors as a result of the same systematic beam offsets from the magnet axis that explain tune and coupling drift.

Table 3 and Table 4 summarize the various feed-down scenarios discussed in this report and show that the observed tune and coupling as well as tune and coupling drifts (Table 1) in the Tevatron can be explained by a combination of the different constant and variable beam offset scenarios developed in section 4). As is obvious from these tables

Analysis of Possible Magnet Related Causes of Tune and Coupling Drift in the Tevatron

there are more mechanisms for $a_1/\Delta a_1$ than for $b_1/\Delta b_1$. The different contributions to $a_1/\Delta a_1$, however, have different signs.

Table 3: Summary of causes for coupling and coupling drift in Tevatron at injection (in magnetic units).

	static	dyn (2 hrs)
Suspension creep	-1	-
Systematic roll of dipoles – scallop beam trajectory ($\Delta y \sim 0.3$ mm)	0.1	0.05
Systematic roll of quadrupoles	?	-
Sag of dipoles (1 mm)	-1	-0.2
Tilt of dipoles (1 mm)	+0.2	-0.05
Sum	-1.7	-0.2
Tevatron - a_1 per dipole	1.4	0.09

Table 4: Summary of causes for tune and tune drift in Tevatron at injection (in magnetic units).

	static	dyn (2 hrs)
Horizontal beam offset (difference betw. b2 correctors and dipoles)	-0.2	-0.07
Dipole sagitta error (1 mm)	1	0
Dipole yaw (1 mm)	0.2	-0.05
Sum	1.0	-0.12
Tevatron - b_1 per dipole	1.4	0.1

References

- 1 M. Martens, G. Annala, "Notes on Tune Drift Measurements at 150 GeV", Fermilab/AD/TEV - Beams-doc-242-v1, 08/21/02, can also be found at http://www-ap.fnal.gov/~martens/tune_drift/tune_drift.html, Another similar (daft) note is M. Martens, G. Annala, W. Fischer, "Measurements of the Tune and Coupling Drifts in the Tevatron on the Injection Front Porch and on the Tevatron Ramp"
- 2 M. Martens, "Measurement of the Tevatron tune shift vs RF frequency and strength of the T:SF and T:SD circuits", Fermilab/AD/TEV - Beams-doc-436, 2002
- 3 M. Martens, B. Hendricks, G. Annala, "Chromaticity, tune and coupling drift and snapback correction algorithms in the Tevatron", Fermilab/AD/TEV - Beams-doc-467, Nov. 2004
- 4 M. Martens, G. Annala, P. Bauer, "Commissioning of the Tune Drift Compensation System", Fermilab/AD/TEV - Beams-doc-475, March 2003
- 5 M. Martens, G. Annala, P. Bauer, "Tune and Coupling Drift Compensation during the Tevatron Injection Porch", presented at the 2003 Particle Accelerator Conference, Portland, May 2003
- 6 M. Martens, P. Bauer, G. Annala, D. Still, G. Velez, "Tevatron chromaticity and tune drift and snapback studies report", Fermilab/AD/TEV - Beams-doc-1236-v1, Jan 2005
- 7 M. Syphers et al., "Strong Transverse Coupling in the Tevatron", Fermilab Beams-Division Internal Note Beams-Doc-501, Exp-203, March 14, 2003
- 8 P. Bauer et al. "Results of an Investigation of the Skew Quadrupole Issue in Tevatron Dipoles", Fermilab internal note TD-03-045, December 2003
- 9 P. Bauer et al., "Tevatron Magnetic Models: Geometric and Hysteretic Multipoles in the Tevatron Dipole", Fermilab Technical Division internal note TD-02-040, Revision 2, May 2004
- 10 G. Velez et al., "Measurements of Geometric, Hysteretic and Dynamic Sextupole in Tevatron Dipoles", Fermilab, Technical Division, internal note TD-04-043, Dec 2004
- 11 R. Berggreen, "Possible Feed-Down of Drift and Snapback Effect in the Skew Quadrupole Coefficient of Tevatron Dipole Magnets", Pre Service Teacher Internship, Pomona College, Fermilab, June 20, 2003
- 12 J. DiMarco, "B0 Drift in Tevatron Dipoles", presentation at the Tevatron department meeting 07/11/2003
- 13 G. Velez, "First Result of Tevatron Quadrupole Measurements", presentation at the tune drift meeting 11/30/2004
- 14 M. J. Syphers, "Effects of Systematic Rolls of Tevatron Magnets," Internal Fermilab Memo, Beams-doc-429, February 11, 2003
- 15 J. Annala, personal communication
- 16 J. Volk et al., "Tevatron alignment issues 2003-2004", Fermilab-Conf-05=040-AD
- 17 M. Martens, "Measured coupling in the Tevatron", Fermilab/AD/TEV - Beams-doc-612-v1, and also in "Notes on the skew Quadrupole Fields in the Tevatron", Fermilab/AD/TEV - Beams-doc-485, March 2003
- 18 D. Harding et al., "Restoring the skew Quadrupole Moment in Tevatron Dipoles", presented at the 2005 Particle Accelerator Conference, Knoxville USA, May 2005
- 19 P. Bauer et al., "Proposals for the Improvement of the Correction of Sextupole Dynamic Effects in Tevatron Dipole Magnets", presented at the European Particle Accelerator Conference, Lucerne June 2004